

hep-ph/9807254

HUPD-9820

SNUTP 98-070

KEK-TH-578

A Model Independent Analysis of the Rare B Decay

$$B \rightarrow X_s l^+ l^-$$

S. Fukae^{a,1}, C. S. Kim^{b,2}, T. Morozumi^{a,3} and T. Yoshikawa^{c,4}*a: Department of Physics, Hiroshima University, Higashi Hiroshima 739-8526, Japan**b: Department of Physics, Yonsei University, Seoul 120-749, Korea**c: Theory Group, KEK, Tsukuba, Ibaraki 305-0801, Japan*

(July 9, 2018)

Abstract

The most general model-independent analysis of the rare B decay, $B \rightarrow X_s l^+ l^-$, is presented. There are ten independent local four-Fermi interactions which may contribute to this process. The branching ratio, the forward-backward asymmetry, and the double differential rate are written as functions of the Wilson coefficients of the ten operators. We also study the correlation between the branching ratio and the forward-backward asymmetry by changing each coefficient. This procedure tells us which types of operator contribute to the process, and it will be very useful to pin down new physics systematically, once we have the experimental data with high statistics and the deviation from the Standard Model is found.

¹fukae@ipc.hiroshima-u.ac.jp²kim@cskim.yonsei.ac.kr, <http://phya.yonsei.ac.kr/~cskim/>³morozumi@theo.phys.sci.hiroshima-u.ac.jp⁴JSPS Research Fellow, yosikawa@theory.kek.jp

1 Introduction

Rare B -meson decays are very useful for constraining new physics beyond the Standard Model (SM). In particular, the processes $B \rightarrow X_s \gamma$ and $B \rightarrow X_s l^+ l^-$ are experimentally clean, and are possibly the most sensitive to the various extensions to the SM because these decays occur only through loops in the SM. Nonstandard model effects can manifest themselves in these rare decays through the Wilson coefficients, which can have values distinctly different from their Standard Model counterparts. (See for example, [1, 2, 3, 4, 5, 6, 7, 8].) Compared to $B \rightarrow X_s \gamma$, the flavor changing leptonic decay $B \rightarrow X_s l^+ l^-$ is more sensitive to the actual form of the new interactions since we can measure experimentally various kinematical distributions as well as a total rate. While new physics will change only the systematically uncertain normalization for $B \rightarrow X_s \gamma$, the interplay of various operators will also change the spectra of the decay $B \rightarrow X_s l^+ l^-$.

We note that the previous studies towards the model independent analysis have been limited to the subset of the ten local four-Fermi interactions within the specific extended models, such as the two-Higgs-doublet model, the minimal supersymmetric model, the left-right symmetric model, and *etc.* (See for example, [4, 9, 10].) In the SM and in many of its extensions, the decay $B \rightarrow X_s l^+ l^-$ is completely determined phenomenologically by the numerical values of Wilson coefficients of only three operators evaluated at the scale $\mu \sim m_b$. However, the most interesting case would be that this three parameter fit is found unsuccessful to explain the real experimental distributions, and that the new interactions necessarily involve an extension of the full operator basis to include new operators beyond the usual set [6]. And, therefore, the new physics scenario can be much richer than any of those models.

In the present paper, instead of doing a model by model analysis, we analyse $B \rightarrow X_s l^+ l^-$ in the most general model-independent way. There are ten types of local four-Fermi interactions which may contribute to the process. This is contrasted to the SM in which there are only two local interactions coming from the Box, γ and Z penguin diagrams and one non-local interaction coming from the cascade decay, $B \rightarrow X_s \gamma^* \rightarrow X_s l^+ l^-$ [11, 12, 13, 14, 15]. Our final purpose is to develop the most general way to distinguish the various four-Fermi interactions, which can be fully investigated at B factories of KEK-B, SLAC-B, B-TeV and LHC-B. As is well known, all results in direct muon decay (energy spectra, polarizations and angular distributions) and in inverse muon decay (the reaction cross section) at energies well below M_W may be parametrized [16] in terms of 10 (complex) couplings, $g_{\alpha\beta}^\gamma$ ($\alpha, \beta = R, L, \gamma = S, V, T$), and the Fermi coupling

constant G_F using the matrix element,

$$\frac{4G_F}{\sqrt{2}} \sum_{\alpha,\beta,\gamma} g_{\alpha\beta}^\gamma < \bar{e}_\alpha | \Gamma^\gamma | \nu_e > < \bar{\nu}_\mu | \Gamma_\gamma | \mu_\beta > . \quad (1)$$

The “ $V - A$ interaction” of the SM corresponds to the single coupling g_{LL}^V , which has been experimentally probed thoroughly.

As quantities to be measured in our first step, we study the decay rate \mathcal{B} and the forward-backward (FB) asymmetry \mathcal{A} [17]. These are written as functions of the coefficients of the interactions, *i.e.*, $\mathcal{B}(\{C_i\})$ and $\mathcal{A}(\{C_i\})$, where $\{C_i\}$ is a set of Wilson coefficients. We study the branching ratio and the FB asymmetry by changing each coefficient. This shows how each operator contributes to the measurements in a different way from the other operators. Furthermore, to distinguish types of operators, we draw the correlation between the decay rate and the asymmetry. By changing each coefficient, we can draw a flow in the two dimensional plane $(\mathcal{B}(C_m), \mathcal{A}(C_m))$ [18]. This flow depends on the type of the interaction which acts. Thus we may see which type of operator contributes to the process once these quantities are measured precisely.

The paper is organized as follows. In Section 2 we show the most general four-Fermi interactions and compute the decay distribution. We also derive the branching ratio and the asymmetry. Their dependence on the four-Fermi interactions is also studied. In Section 3 the correlation between the branching ratio and the asymmetry is discussed and Section 4 is devoted to our summary.

2 The four-Fermi interactions and the decay distributions

We start by defining the various kinematic variables. In the present paper, the inclusive semileptonic B decay is modeled by the partonic calculation, *i.e.*, $b(p_b) \rightarrow s(p_s) + l^+(p_+) + l^-(p_-)$. This is regarded as the leading order calculation in the $1/m_b$ expansion [19, 20]. Then the decay distribution is described by the following two kinematic variables s and u ,

$$\begin{aligned} s &= (p_b - p_s)^2 = (p_+ + p_-)^2 = m_b^2 + m_s^2 + m_+^2 + m_-^2 - t_+ - t_-, \\ t_+ &= (p_s + p_+)^2 = (p_b - p_-)^2, \\ t_- &= (p_s + p_-)^2 = (p_b - p_+)^2, \\ u &= t_+ - t_-. \end{aligned} \quad (2)$$

In the center of mass frame of the dileptons, u is written in terms of θ , *i.e.*, the angle between the momentum of the B meson and that of l^+ ,

$$\begin{aligned} u &= -u(s) \cdot \cos\theta \equiv -u(s)z, \\ \text{with } z &= \cos\theta, \\ u(s) &= \sqrt{(s - (m_b + m_s)^2)(s - (m_b - m_s)^2)(1 - \frac{4m_l^2}{s})}. \end{aligned} \quad (3)$$

The phase space is defined in terms of s and z ,

$$\begin{aligned} 4m_l^2 &\leq s \leq (m_b - m_s)^2, \\ -1 &\leq z \leq 1. \end{aligned} \quad (4)$$

The matrix element of the decay is written as the sum of the SM contribution and the contribution from the local four-Fermi interactions,

$$\mathcal{M} = \mathcal{M}_{\text{SM}} + \mathcal{M}_{\text{NEW}}, \quad (5)$$

where \mathcal{M}_{SM} is the SM part and is given by

$$\begin{aligned} \mathcal{M}_{\text{SM}} = \frac{G_F \alpha}{\sqrt{2}\pi} V_{ts}^* V_{tb} \quad [& (C_9^{\text{eff}} - C_{10}) \bar{s}_L \gamma_\mu b_L \bar{l}_L \gamma^\mu l_L \\ & + (C_9^{\text{eff}} + C_{10}) \bar{s}_L \gamma_\mu b_L \bar{l}_R \gamma^\mu l_R \\ & - 2C_7^{\text{eff}} \bar{s} i \sigma_{\mu\nu} \frac{q^\nu}{q^2} (m_s L + m_b R) b \bar{l} \gamma^\mu l], \end{aligned} \quad (6)$$

We use the following values for the Wilson coefficients ($C_9^{\text{NDR}} = 4.153, C_{10} = -4.546, C_7 = -0.311$). They correspond to the next-to leading calculation of QCD corrections [14, 15]. The renormalization point μ and the top quark mass are set to be $\mu = m_b = 4.8$ (GeV) and $m_t = 175$ (GeV), unless otherwise specified. (We follow Ref. [21] for the choice of the parameters in the SM as well as the incorporation of the long-distance effects of charmonium states [22, 23].) There are ten independent local four-Fermi interactions which may contribute to the process. \mathcal{M}_{NEW} is a function of the coefficients of local four-Fermi interactions and is defined as

$$\begin{aligned} \mathcal{M}_{\text{NEW}} = \frac{G_F \alpha}{\sqrt{2}\pi} V_{ts}^* V_{tb} \quad [& C_{LL} \bar{s}_L \gamma_\mu b_L \bar{l}_L \gamma^\mu l_L \\ & + C_{LR} \bar{s}_L \gamma_\mu b_L \bar{l}_R \gamma^\mu l_R \\ & + C_{RL} \bar{s}_R \gamma_\mu b_R \bar{l}_L \gamma^\mu l_L \\ & + C_{RR} \bar{s}_R \gamma_\mu b_R \bar{l}_R \gamma^\mu l_R \\ & + C_{LRLR} \bar{s}_L b_R \bar{l}_L l_R \end{aligned}$$

$$\begin{aligned}
& + C_{RLLR} \bar{s}_R b_L \bar{l}_L l_R \\
& + C_{LRRL} \bar{s}_L b_R \bar{l}_R l_L \\
& + C_{RLRL} \bar{s}_R b_L \bar{l}_R l_L \\
& + C_T \bar{s} \sigma_{\mu\nu} b \bar{l} \sigma^{\mu\nu} l \\
& + i C_{TE} \bar{s} \sigma_{\mu\nu} b \bar{l} \sigma_{\alpha\beta} l \epsilon^{\mu\nu\alpha\beta}, \tag{7}
\end{aligned}$$

where the C_X 's are the coefficients of four-Fermi interactions. Among them, there are four vector type interactions denoted by C_{LL} , C_{LR} , C_{RL} , and C_{RR} . Two of them (C_{LL} , C_{LR}) are already present in the SM as the combinations of $(C_9 - C_{10}, C_9 + C_{10})$. Therefore they correspond to the deviation of these coefficients from the SM values. The other interactions, denoted by C_{RL} and C_{RR} , are obtained by interchanging the chirality projections L and R . There are four scalar type interactions, C_{LRLR} , C_{RLLR} , C_{RLLR} , and C_{RLRL} . The remaining two, denoted by C_T and C_{TE} , correspond to tensor type.

It is now straightforward to compute the double differential decay rate. The results for the massless lepton case, $B \rightarrow X_s e^+ e^-$ and $B \rightarrow X_s \mu^+ \mu^-$, are explicitly written in the text. The massive case is separately given in the Appendix. The double differential rate is a function of the dilepton invariant mass s and $z = \cos \theta$. In the massless limit, the interference between tensor (scalar) type interactions and vector type interactions vanishes. Then the expression becomes considerably simplified,

$$\begin{aligned}
\frac{d\mathcal{B}}{dsdz} &= \frac{1}{2m_b^8} \mathcal{B}_0 \quad [\quad A_1(s, z) \{4|C_7|^2\} \\
& + A_2(s, z) \{ |(C_9^{eff} - C_{10})|^2 + |(C_9^{eff} + C_{10})|^2 \} \\
& + A_3(s, z) \{ |(C_9^{eff} - C_{10})|^2 - |(C_9^{eff} + C_{10})|^2 \} \\
& + A_4(s, z) \{ 2Re(-2C_7(C_9^{eff*} - C_{10}^*)) + 2Re(-2C_7(C_9^{eff*} + C_{10}^*)) \} \\
& + A_5(s, z) \{ 2Re(-2C_7(C_9^{eff*} - C_{10}^*)) - 2Re(-2C_7(C_9^{eff*} + C_{10}^*)) \} \\
& + A_2(s, z) \{ 2Re((C_9^{eff} - C_{10})\mathbf{C}_{\mathbf{LL}}^*) + 2Re((C_9^{eff} + C_{10})\mathbf{C}_{\mathbf{LR}}^*) \} \\
& + A_3(s, z) \{ 2Re((C_9^{eff} - C_{10})\mathbf{C}_{\mathbf{LL}}^*) - 2Re((C_9^{eff} + C_{10})\mathbf{C}_{\mathbf{LR}}^*) \} \\
& + A_4(s, z) \{ 2Re(-2C_7(\mathbf{C}_{\mathbf{LL}}^* + \mathbf{C}_{\mathbf{LR}}^*)) \} \\
& + A_5(s, z) \{ 2Re(-2C_7(\mathbf{C}_{\mathbf{LL}}^* - \mathbf{C}_{\mathbf{LR}}^*)) \} \\
& + A_6(s, z) \{ 2Re(-2C_7(\mathbf{C}_{\mathbf{RL}}^* + \mathbf{C}_{\mathbf{RR}}^*)) \} \\
& + A_6(s, z) \{ -2Re((C_9^{eff} - C_{10})\mathbf{C}_{\mathbf{RL}}^*) - 2Re((C_9^{eff} + C_{10})\mathbf{C}_{\mathbf{RR}}^*) \}
\end{aligned}$$

$$\begin{aligned}
& + A_7(s, z) \{2\text{Re}(-2C_7(\mathbf{C}_{\mathbf{RL}}^* - \mathbf{C}_{\mathbf{RR}}^*))\} \\
& + A_2(s, z) \{|\mathbf{C}_{\mathbf{LL}}|^2 + |\mathbf{C}_{\mathbf{LR}}|^2 + |\mathbf{C}_{\mathbf{RL}}|^2 + |\mathbf{C}_{\mathbf{RR}}|^2\} \\
& + A_3(s, z) \{|\mathbf{C}_{\mathbf{LL}}|^2 - |\mathbf{C}_{\mathbf{LR}}|^2 - |\mathbf{C}_{\mathbf{RL}}|^2 + |\mathbf{C}_{\mathbf{RR}}|^2\} \\
& + A_3(s, z) \{-4\text{Re}[\mathbf{C}_{\mathbf{LRLR}}(\mathbf{C}_{\mathbf{T}}^* - 2\mathbf{C}_{\mathbf{TE}}^*) + \mathbf{C}_{\mathbf{RLRL}}(\mathbf{C}_{\mathbf{T}}^* + 2\mathbf{C}_{\mathbf{TE}}^*)]\} \\
& + A_6(s, z) \{-2\text{Re}(\mathbf{C}_{\mathbf{LL}}\mathbf{C}_{\mathbf{RL}}^* + \mathbf{C}_{\mathbf{LR}}\mathbf{C}_{\mathbf{RR}}^*) \\
& \quad + \text{Re}(\mathbf{C}_{\mathbf{LRLR}}\mathbf{C}_{\mathbf{RLLR}}^* + \mathbf{C}_{\mathbf{LRRL}}\mathbf{C}_{\mathbf{RLRL}}^*)\} \\
& + A_8(s, z) \{|\mathbf{C}_{\mathbf{LRLR}}|^2 + |\mathbf{C}_{\mathbf{RLLR}}|^2 + |\mathbf{C}_{\mathbf{LRRL}}|^2 + |\mathbf{C}_{\mathbf{RLRL}}|^2\} \\
& + A_9(s, z) \{16|\mathbf{C}_{\mathbf{T}}|^2 + 64|\mathbf{C}_{\mathbf{TE}}|^2\}, \tag{8}
\end{aligned}$$

where A_n are the functions of kinematic variables s and z ,

$$A_1(s, z) = \frac{1}{s}u(s)\{-16m_b^2m_s^2s + (m_b^2 + m_s^2)(-2s^2 + 2u(s)^2z^2 + 2(m_b^2 - m_s^2)^2)\}, \tag{9}$$

$$A_2(s, z) = u(s)\{-u(s)^2z^2 - s^2 + (m_b^2 - m_s^2)^2\}, \tag{10}$$

$$A_3(s, z) = 2u(s)^2zs, \tag{11}$$

$$A_4(s, z) = u(s)\{2(m_b^2 + m_s^2)s - 2(m_b^2 - m_s^2)^2\}, \tag{12}$$

$$A_5(s, z) = -2(m_b^2 + m_s^2)u(s)^2z, \tag{13}$$

$$A_6(s, z) = 4m_b m_s s u(s), \tag{14}$$

$$A_7(s, z) = 4m_b m_s u(s)^2z, \tag{15}$$

$$A_8(s, z) = u(s)(m_b^2 + m_s^2 - s)s, \tag{16}$$

$$A_9(s, z) = u(s)\{-2u(s)^2z^2 - 2s(m_b^2 + m_s^2) + 2(m_b^2 - m_s^2)^2\}, \tag{17}$$

$$u(s) = \sqrt{\{s - (m_b - m_s)^2\}\{s - (m_b + m_s)^2\}}. \tag{18}$$

Among them, $A_1, A_2, A_4, A_6, A_8, A_9$ are even functions with respect to z while A_3, A_5 , and A_7 are odd functions with respect to z . The former contribute to the single differential rate $d\mathcal{B}/ds$ and the latter contributes to the forward-backward (FB) asymmetry $d\mathcal{A}/ds$.

Let us first investigate the single differential rate,

$$\frac{d\mathcal{B}}{ds} = \int_{-1}^1 \frac{d^2\mathcal{B}}{dsdz} dz. \tag{19}$$

It is given by

$$\begin{aligned}
\frac{d\mathcal{B}}{ds}(s) = \frac{1}{2m_b^8}\mathcal{B}_0 \quad [& M_1(s) \{4|C_7|^2\} \\
& + M_2(s) \{2|C_9^{eff}|^2 + 2|C_{10}|^2\}
\end{aligned}$$

$$\begin{aligned}
& +2Re(C_9^{eff}(C_{LL}^* + C_{LR}^*)) + 2Re(C_{10}(-C_{LL}^* + C_{LR}^*)) \\
& + |C_{LL}|^2 + |C_{LR}|^2 + |C_{RL}|^2 + |C_{RR}|^2\} \\
- & M_4(s) \{4Re[C_7^*(2C_9^{eff} + C_{LL} + C_{LR})]\} \\
- & M_6(s) \{4Re[C_7^*(C_{RL} + C_{RR})] \\
& + 2Re(C_9^{eff}(C_{RL}^* + C_{RR}^*)) + 2Re(C_{10}(-C_{RL}^* + C_{RR}^*)) \\
& + 2Re(C_{LL}C_{RL}^* + C_{LR}C_{RR}^*) - Re(C_{LRLR}C_{RLLR}^* + C_{LRRL}C_{RLRL}^*)\} \\
+ & M_8(s) \{|C_{LRLR}|^2 + |C_{RLLR}|^2 + |C_{LRRL}|^2 + |C_{RLRL}|^2\} \\
+ & M_9(s) \{16|C_T|^2 + 64|C_{TE}|^2\}, \tag{20}
\end{aligned}$$

where \mathcal{B}_0 is a normalization factor,

$$\mathcal{B}_0 = \mathcal{B}_{sl} \frac{3\alpha^2}{16\pi^2} \frac{|V_{ts}^* V_{tb}|^2}{|V_{cb}|^2} \frac{1}{f(\hat{m}_c) \kappa(\hat{m}_c)}, \tag{21}$$

and the phase space factor, $f(\hat{m}_c = \frac{m_c}{m_b})$, and the $O(\alpha_s)$ QCD correction factor [24], $\kappa(\hat{m}_c)$, of $b \rightarrow cl\nu$ are given by

$$f(\hat{m}_c) = 1 - 8\hat{m}_c^2 + 8\hat{m}_c^6 - \hat{m}_c^8 - 24\hat{m}_c^4 \ln \hat{m}_c, \tag{22}$$

$$\kappa(\hat{m}_c) = 1 - \frac{2\alpha_s(m_b)}{3\pi} \left[\left(\pi^2 - \frac{31}{4} \right) (1 - \hat{m}_c)^2 + \frac{3}{2} \right]. \tag{23}$$

For the numerical calculations, we set $\frac{|V_{ts}^* V_{tb}|^2}{|V_{cb}|^2} = 1$ and use $\mathcal{B}_{sl} = 10.4\%$. M_n are functions which are obtained by integrating $A_n(s, z)$ with respect to z as follows,

$$M_n(s) = \int_{-1}^1 A_n(s, z) dz = 2A_n(s, \sqrt{1/3}), \tag{24}$$

where n is 1,2,4,6,8 and 9 and they are explicitly given by

$$M_1(s) = 2u(s) \frac{1}{s} [-16m_b^2 m_s^2 s + (m_b^2 + m_s^2)(-2s^2 + \frac{2}{3}u(s)^2 + 2(m_b^2 - m_s^2)^2)], \tag{25}$$

$$M_2(s) = -2u(s) [\frac{1}{3}u(s)^2 + s^2 - (m_b^2 - m_s^2)^2], \tag{26}$$

$$M_4(s) = 2u(s) [2(m_b^2 + m_s^2)s - 2(m_b^2 - m_s^2)^2], \tag{27}$$

$$M_6(s) = 2u(s) [4m_b m_s s], \tag{28}$$

$$M_8(s) = 2u(s) [s(m_b^2 + m_s^2 - s)], \tag{29}$$

$$M_9(s) = 2u(s) [-\frac{2}{3}u(s)^2 - 2(m_b^2 + m_s^2)s + 2(m_b^2 - m_s^2)^2]. \tag{30}$$

In order to compare the kinematic functions M_n , we plot them in Figure 1. This plot shows that M_1 is the largest due to its $1/s$ dependence and that M_6 is suppressed by a factor of m_s

(the strange quark mass). Knowing the kinematical dependence, we plot the differential decay rate $d\mathcal{B}/ds$ by changing each coefficient C_X in the new physics amplitude \mathcal{M}_{NEW} . We summarize how the differential rate $d\mathcal{B}/ds$ is changed accordingly.

- **Vector type interactions**

We assume that C_X are real parameters. This means we do not introduce any new physics phase in addition to that of the SM given by $\text{Arg}(V_{ts}^* V_{tb})$. In Figs. 2,3,4 and 5, we change $C_{LL}, C_{LR}, C_{RL}, C_{RR}$ respectively. Among the vector interactions, $d\mathcal{B}/ds$ changes the most with respect to C_{LL} . This can be explained as follows. By neglecting the term proportional to M_6 , we can collect the terms coming from C_{LL}, C_{LR}, C_{RL} , and C_{RR} . They are given by

$$M_2(s)C_{LL}^2 + \{M_2(s)2(C_9^{eff} - C_{10}) + M_4(s)(-4C_7)\}C_{LL}, \quad (31)$$

$$M_2(s)C_{LR}^2 + \{M_2(s)2(C_9^{eff} + C_{10}) + M_4(s)(-4C_7)\}C_{LR}, \quad (32)$$

$$M_2(s)C_{RL}^2, \quad (33)$$

$$M_2(s)C_{RR}^2. \quad (34)$$

Around $s = 5 \text{ GeV}^2$, $\text{Re}(C_9^{eff} - C_{10}) \sim 9.5$ and $\text{Re}(C_9^{eff} + C_{10}) \sim 0.4$. Then the interference term between C_{LL} and $\text{Re}(C_9^{eff} - C_{10})$ is large and $d\mathcal{B}/ds$ is sensitive to the change of C_{LL} . The contribution is constructive for $C_{LL} = |C_{10}|$ and destructive for $C_{LL} = -|C_{10}|$, as shown in Figure 1. The effects of the other vector interactions (C_{LR}, C_{RR}, C_{RL}) are smaller than that of C_{LL} . To see this dependence clearly, we have also studied the partially integrated branching ratio (\mathcal{B}) and have shown how it depends on the coefficients. (See Figures 8 and 9.) The range for the integration is $1 \leq s \leq 8 \text{ (GeV}^2\text{)}$. This range is below the J/ψ resonance and $d\mathcal{B}/ds$ is nearly flat within the range. From these figures, the branchingratio depends strongly on C_{LL} while the dependence on the other coefficients is rather weak. The contribution of C_{LL} to \mathcal{B} is positive (negative) for $C_{LL} > 0$ (< 0). The contribution due to C_{RL} and C_{RR} is positive.

- **Scalar and tensor type interactions**

The scalar and tensor interactions increase $d\mathcal{B}/ds$, as shown in Figures 6 and 7. This can be interpreted as follows. As far as we see the sensitivity to only one of the scalar operators, *i.e.*, $C_{LRLR}, C_{RLLR}, C_{LRRL}$ and C_{RLRL} , the interference term does not act at all. And it is enough to study the response of $d\mathcal{B}/ds$ to the change of the combinations of the coefficients, $|C_{LRLR}|^2 + |C_{RLLR}|^2 + |C_{LRRL}|^2 + |C_{RLRL}|^2$ and $16|C_T|^2 + 64|C_{TE}|^2$. Because their contribution is always positive, it increases $d\mathcal{B}/ds$. Furthermore, even if two

or more scalar interactions act together, the effect of the interference term denoted by M_6 is suppressed by a factor of m_s and can not exceed the positive contribution. Thus the major dependence on the coefficients comes through the combination, $|C_{LRLR}|^2 + |C_{RLLR}|^2 + |C_{LRRL}|^2 + |C_{RLRL}|^2$, even if two or more operators contribute to the process. Therefore, $d\mathcal{B}/ds$ increases even if more than one scalar and/or tensor type of interaction are present. In Figures 8 and 9, we can see that the branching ratio \mathcal{B} always increases as one of the scalar and tensor interactions act.

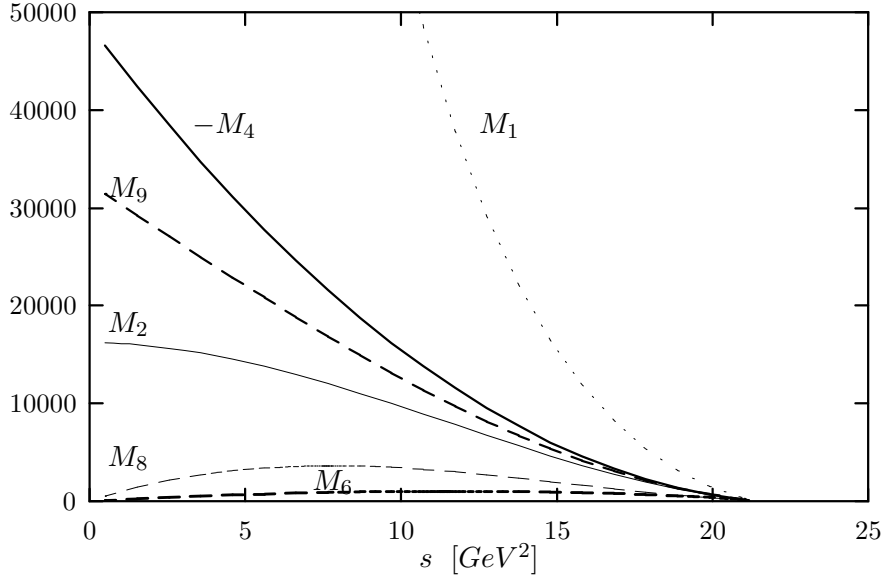


Figure 1 $M_1(s)$ (thin dotted line), $M_2(s)$ (thin solid line), $-M_4(s)$ (thick solid line), $M_6(s)$ (thick dashed line), $M_8(s)$ (thin dashed line) and $M_9(s)$ (dashed line).

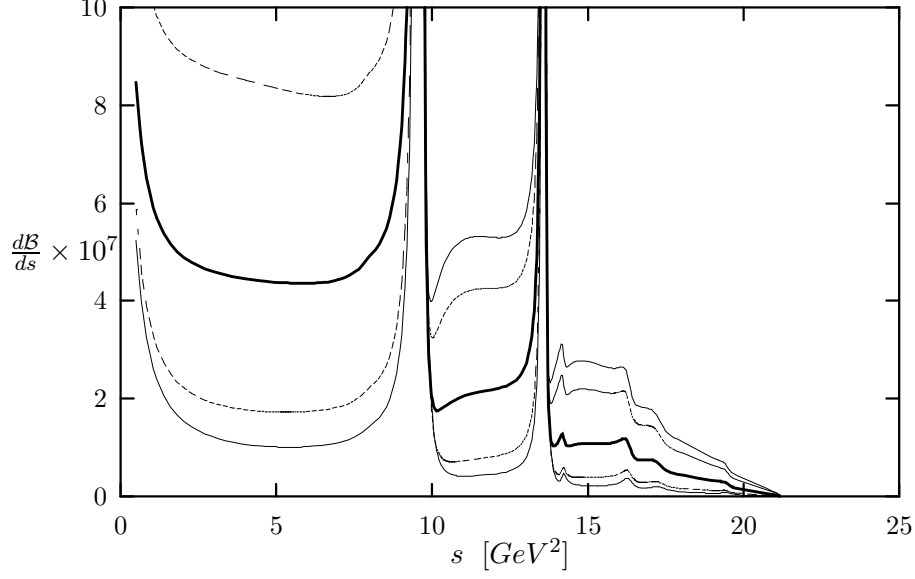


Figure 2 The differential branching ratio for the SM (thick solid line), C_{LL} is $-|C_{10}|$ (thin line), $-0.7|C_{10}|$ (thin dashed line), $0.7|C_{10}|$ (thin dashed line) and $|C_{10}|$ (thin line). The coefficients of the other interactions in \mathcal{M}_{NEW} are set to zero.

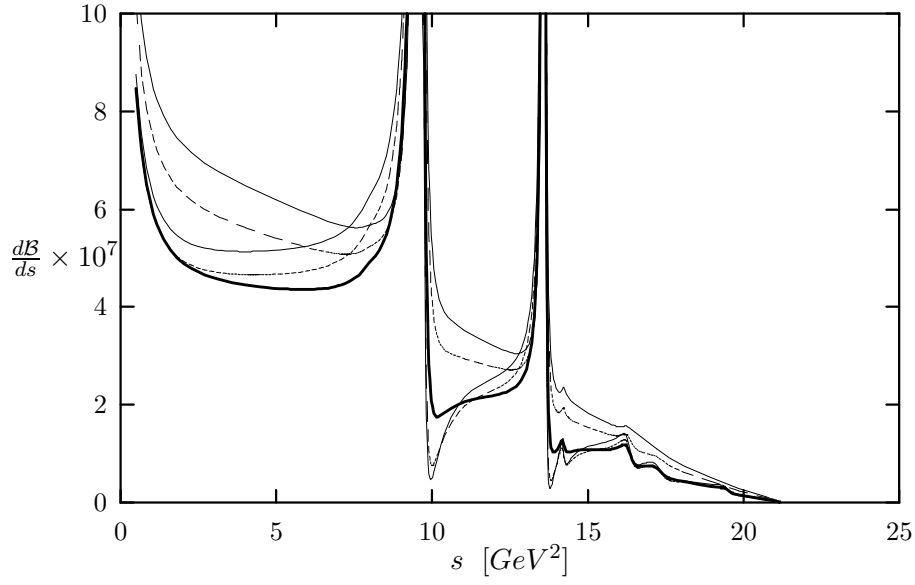


Figure 3 The differential branching ratio for the SM (thick solid line), C_{LR} is $-|C_{10}|$ (thin line), $-0.7|C_{10}|$ (thin dashed line), $0.7|C_{10}|$ (thin dashed line) and $|C_{10}|$ (thin line). The coefficients of the other interactions in \mathcal{M}_{NEW} are set to zero.

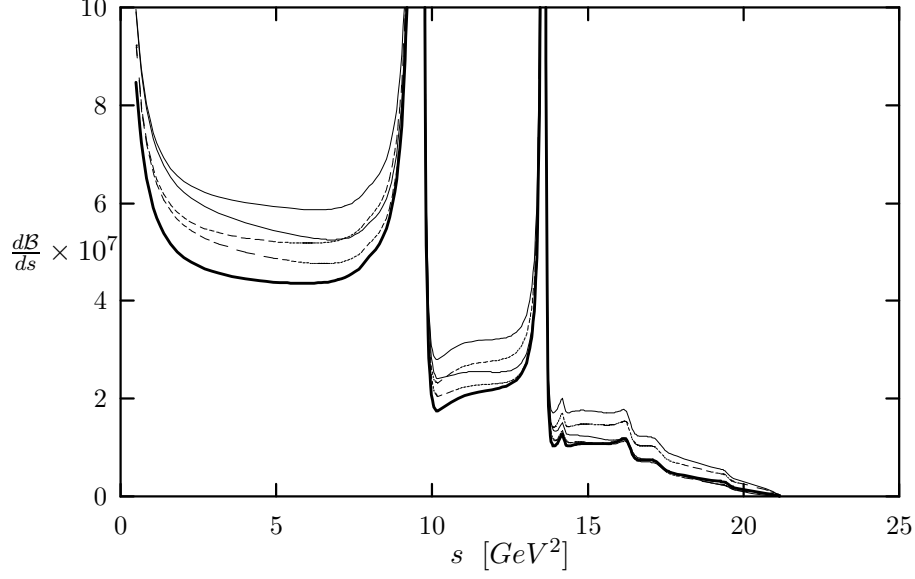


Figure 4 The differential branching ratio for the SM (thick solid line), C_{RL} is $-|C_{10}|$ (thin line), $-0.7|C_{10}|$ (thin dashed line), $0.7|C_{10}|$ (thin dashed line) and $|C_{10}|$ (thin line). The coefficients of the other interactions in \mathcal{M}_{NEW} are set to zero.

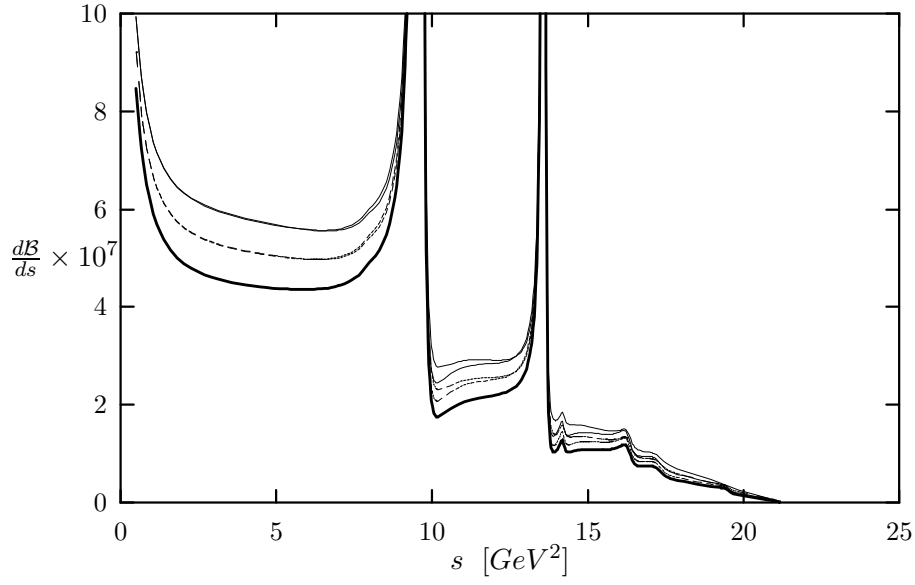


Figure 5 The differential branching ratio for the SM (thick solid line), C_{RR} is $-|C_{10}|$ (thin line), $-0.7|C_{10}|$ (thin dashed line), $0.7|C_{10}|$ (thin dashed line) and $|C_{10}|$ (thin line). The coefficients of the other interactions in \mathcal{M}_{NEW} are set to zero.

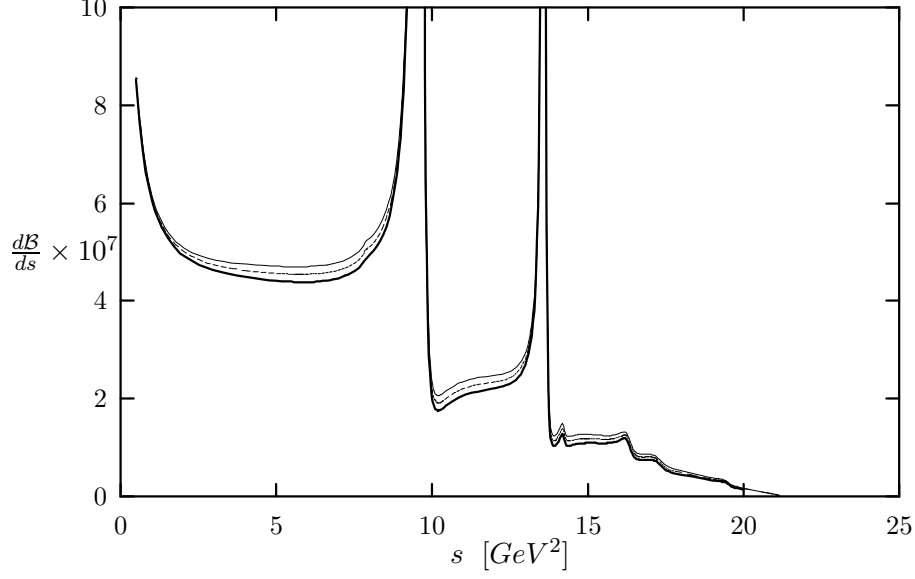


Figure 6 The differential branching ratio for the SM (thick solid line), $|C_{LRLR}|^2 + |C_{RLLR}|^2 + |C_{LRRL}|^2 + |C_{RLRL}|^2 = 0.5 |C_{10}|^2$ (thin dashed line) and $|C_{10}|^2$ (thin solid line).

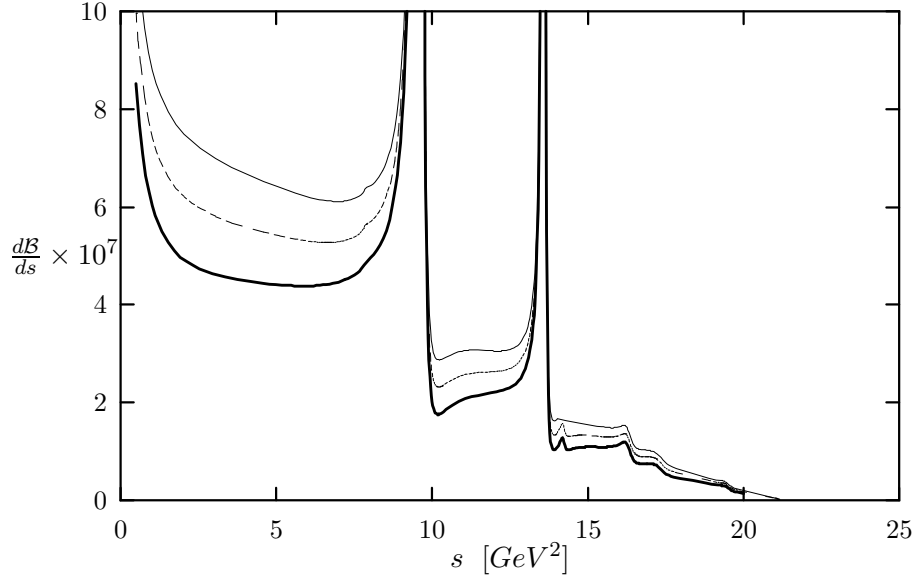


Figure 7 The differential branching ratio for the SM (thick solid line), $16 |C_T|^2 + 64 |C_{TE}|^2 = 0.5 |C_{10}|^2$ (thin dashed line) and $|C_{10}|^2$ (thin solid line).

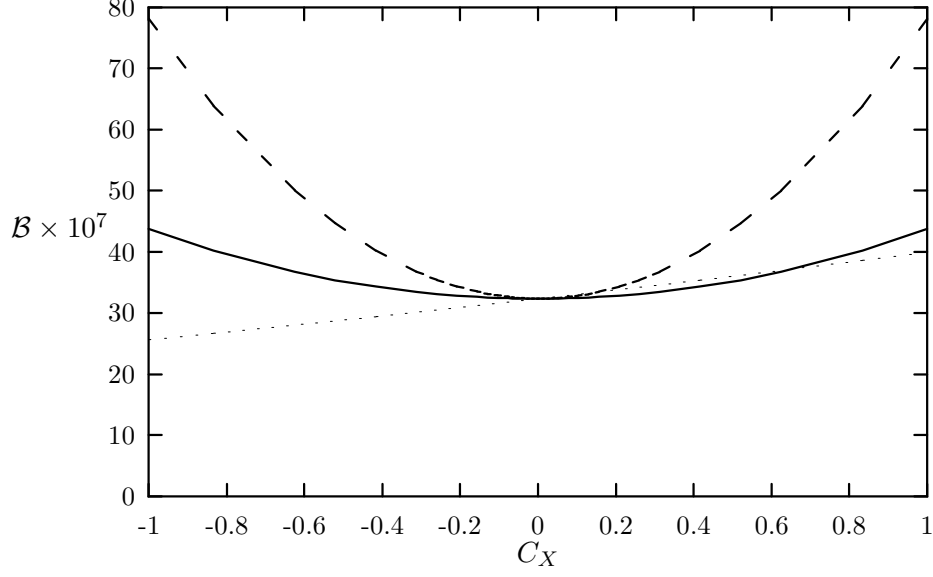


Figure 8 The partially integrated branching ratio $\mathcal{B} = \int_1^8 \frac{d\mathcal{B}}{ds} ds$ as a function of C_T (thick line), C_{TE} (thick dashed line) and C_{LL} (dotted dashed line).

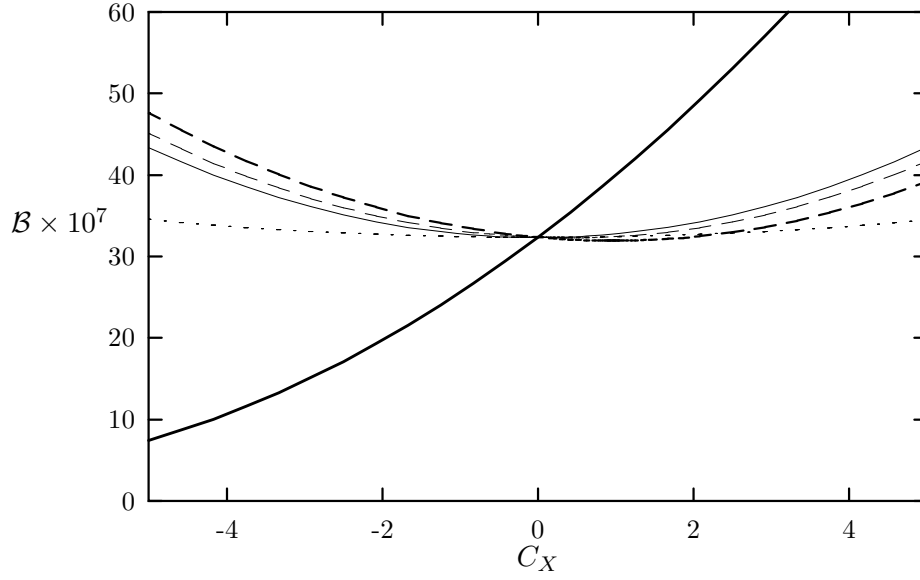


Figure 9 The partially integrated branching ratio $\mathcal{B} = \int_1^8 \frac{d\mathcal{B}}{ds} ds$ as a function of C_{LL} (thick solid line), C_{LR} (thick dashed line), C_{RL} (thin dashed line), C_{RR} (thin solid line) and C_{LRRL} (dotted line).

Now let us turn to the forward-backward (FB) asymmetry. The normalized asymmetry $d\bar{\mathcal{A}}/ds$ is given by

$$\frac{d\bar{\mathcal{A}}}{ds} = \frac{\frac{d\mathcal{A}}{ds}}{\frac{d\mathcal{B}}{ds}} = \frac{\int_0^1 dz \frac{d^2\mathcal{B}}{dsdz} - \int_{-1}^0 dz \frac{d^2\mathcal{B}}{dsdz}}{\int_0^1 dz \frac{d^2\mathcal{B}}{dsdz} + \int_{-1}^0 dz \frac{d^2\mathcal{B}}{dsdz}}, \quad (35)$$

where $\frac{d\mathcal{A}}{ds}$ is the FB asymmetry and is expressed as

$$\begin{aligned} \frac{d\mathcal{A}}{ds} = \frac{1}{2m_b^8} \mathcal{B}_0 \quad [& A_3(s, 1) \{ |(C_9^{eff} - C_{10})|^2 - |(C_9^{eff} + C_{10})|^2 \} \\ & + A_5(s, 1) \{ 2\text{Re}(-2C_7(C_9^{eff*} - C_{10}^*)) - 2\text{Re}(-2C_7(C_9^{eff*} + C_{10}^*)) \} \\ & + A_3(s, 1) \{ 2\text{Re}((C_9^{eff} - C_{10})C_{LL}^*) - 2\text{Re}((C_9^{eff} + C_{10})C_{LR}^*) \} \\ & + A_5(s, 1) \{ 2\text{Re}(-2C_7(C_{LL}^* - C_{LR}^*)) \} \\ & + A_7(s, 1) \{ 2\text{Re}(-2C_7(C_{RL}^* - C_{RR}^*)) \} \\ & + A_3(s, 1) \{ |C_{LL}|^2 - |C_{LR}|^2 - |C_{RL}|^2 + |C_{RR}|^2 \} \\ & + A_3(s, 1) \{ -4\text{Re}[C_{LRLR}(C_T^* - 2C_{TE}^*) + C_{RLRL}(C_T^* + 2C_{TE}^*)] \} \}. \end{aligned} \quad (36)$$

$A_n(s, 1)$ are the functions which are obtained by integrating $A_n(s, z)$ with respect to z ,

$$A_n(s, 1) = \int_0^1 A_n(s, z) dz - \int_{-1}^0 A_n(s, z) dz, \quad (37)$$

$$A_3(s, 1) = 2u(s)^2 s, \quad (38)$$

$$A_5(s, 1) = -2(m_b^2 + m_s^2)u(s)^2, \quad (39)$$

$$A_7(s, 1) = 4m_b m_s u(s)^2, \quad (40)$$

where n is 3, 5 and 7. These kinematic functions are plotted in Figure 10. Among them, A_7 is smaller than the others because it is suppressed by a factor of m_s . In the same way as we have done for the differential rate, we plot the normalized asymmetry by changing a coefficient of vector type interactions within the range $-C_{10} < C_X < C_{10}$. The results are shown in Figures 11-14. These plots show that the asymmetry is the most sensitive to C_{LL} , which gives a positive (negative) contribution for $C_{LL} > 0$ (< 0). Figures 13 and 14 tell us that C_{RL} (C_{RR}) decreases (increases) the asymmetry. To interpret the results, we collect the terms coming from a vector type interaction in the FB asymmetry,

$$A_3(s) \{ C_{LL}^2 + 2(C_9^{eff} - C_{10})C_{LL} \} - 4A_5(s)C_7C_{LL}, \quad (41)$$

$$A_3(s)\{-C_{LR}^2 - 2(C_9^{eff} + C_{10})C_{LR}\} + 4A_5(s)C_7C_{LR}, \quad (42)$$

$$A_3(s)\{-C_{RL}^2\}, \quad (43)$$

$$A_3(s)\{C_{RR}^2\}, \quad (44)$$

where we neglect the term proportional to A_7 . Because $(C_9^{eff} - C_{10})$ is much larger than the other SM coefficients, the interference term with C_{LL} is important. Therefore the asymmetry is sensitive to C_{LL} . The response to C_{LR} is more involved and the interference term between C_7 and C_{LR} seems to be the most important. It gives a positive (negative) contribution to the asymmetry for $C_{LR} > 0$ (< 0). We also note that C_{RL} (C_{RR}) gives a negative (positive) contribution to the asymmetry and it is consistent with the results shown in Figures 13 and 14.

We now study the integrated FB asymmetry (\mathcal{A}). We choose the same integration region as was chosen for the branching ratio (\mathcal{B}), and define the integrated FB asymmetry \mathcal{A} and the normalized FB asymmetry $\bar{\mathcal{A}}$,

$$\mathcal{A} = \int_1^8 \frac{d\mathcal{A}}{ds} ds, \quad (45)$$

$$\bar{\mathcal{A}} = \int_1^8 \frac{d\mathcal{A}}{ds} ds / \mathcal{B}, \quad (46)$$

where $\mathcal{B} = \int_1^8 \frac{d\mathcal{B}}{ds} ds$. We outline how \mathcal{A} and $\bar{\mathcal{A}}$ depend on the interactions. In Figure 15 (16), the dependence of the integrated asymmetry \mathcal{A} (normalized asymmetry $\bar{\mathcal{A}}$) on $|C_X|$ is shown by changing the coefficient $|C_X|$ within the small range, $-C_{10} < |C_X| < C_{10}$. Within this range, the linear dependence on the coefficients is important. At first glance, we see that only C_{LL} can give rise to both large positive and negative contributions. C_{LR} also gives rise to both positive and negative contributions. C_{RR} gives a positive contribution and C_{RL} gives a negative contribution as already discussed for $d\mathcal{A}/ds$. We also note that the integrated FB asymmetry does not change at all as we change a coefficient of one of the scalar or tensor interactions. (See Figure 15.) This is because the dependence on these types of interactions comes only from the interference term. On the other hand, the magnitude of the averaged FB asymmetry is reduced slightly if one of these interactions act. The reason is that the denominator of the averaged FB asymmetry, \mathcal{B} , always increases as scalar and tensor interactions are switched on.

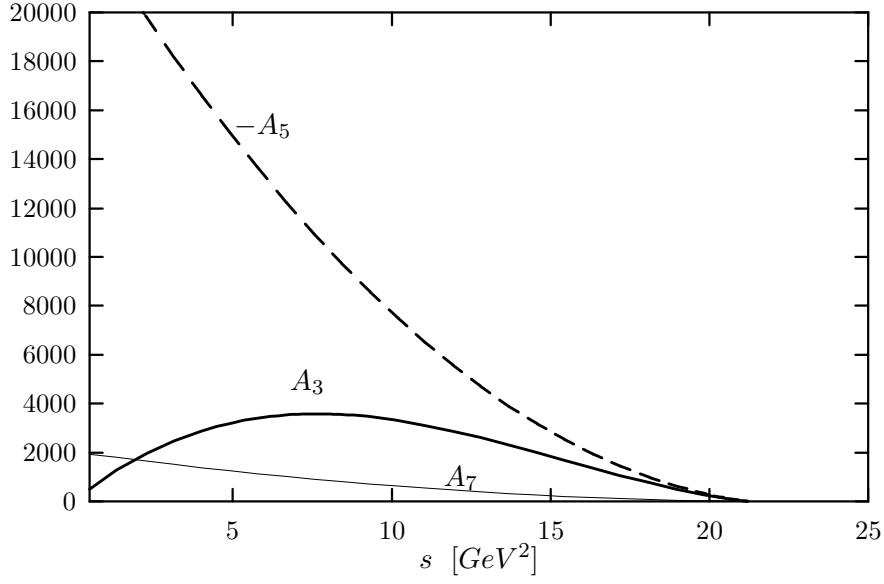


Figure 10 $A_3(s, 1)$ (thin dotted line), $-A_5(s, 1)$ (thin solid line) and $A_7(s, 1)$ (thick solid line).

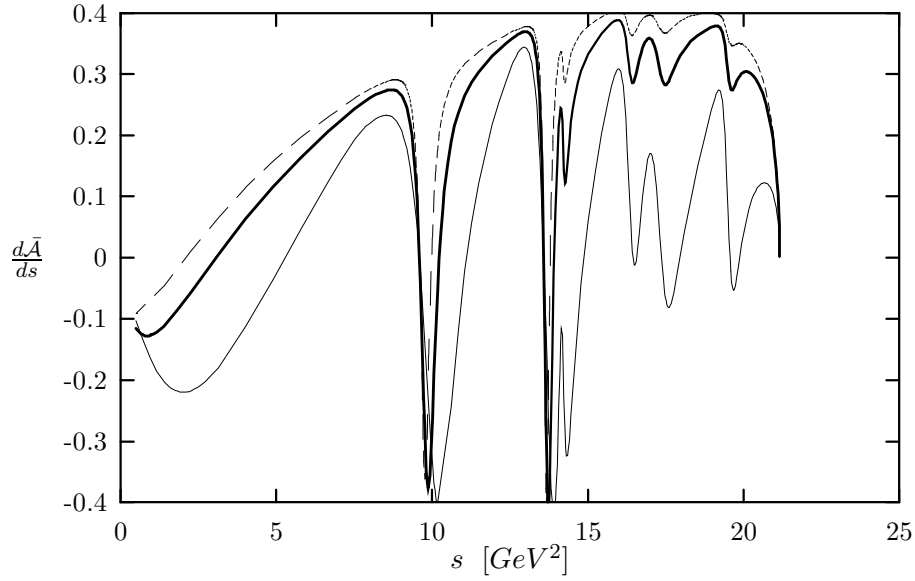


Figure 11 The normalized FB asymmetry for the SM (thick solid line), C_{LL} is $-|C_{10}|$ (thin line) and $|C_{10}|$ (thin dashed line). The coefficients of the other interactions in \mathcal{M}_{NEW} are set to zero.

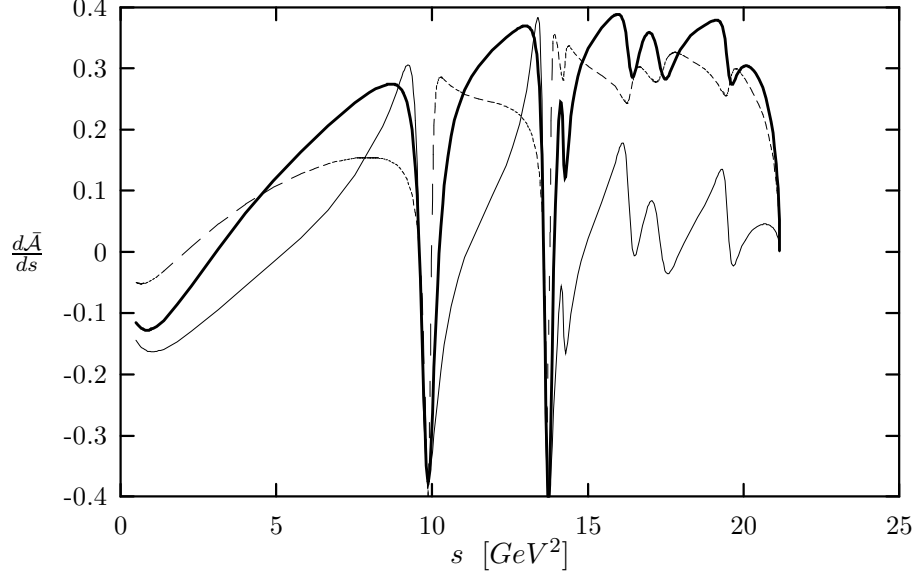


Figure 12 The normalized FB asymmetry for the SM (thick solid line), C_{LR} is $-|C_{10}|$ (thin line) and $|C_{10}|$ (thin dashed line). The coefficients of the other interactions in \mathcal{M}_{NEW} are set to zero.

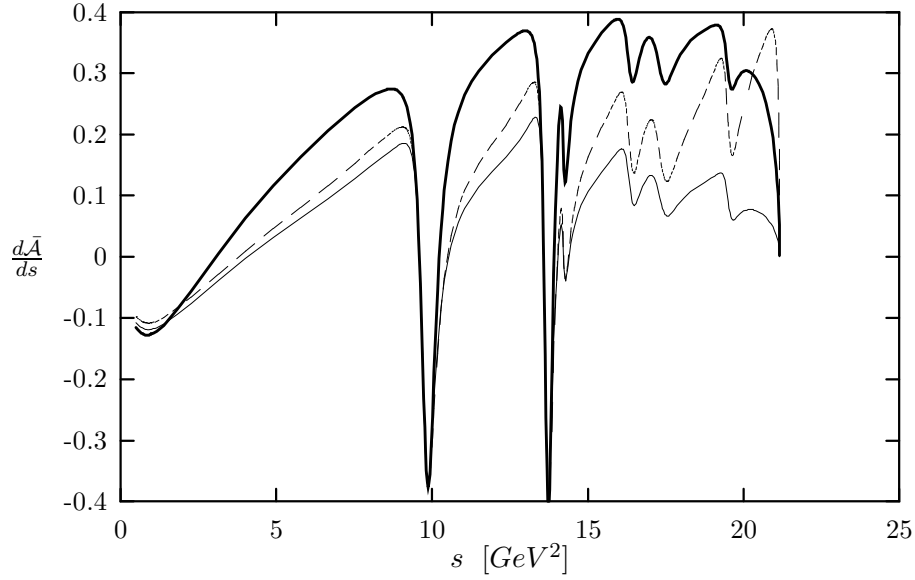


Figure 13 The normalized FB asymmetry for the SM (thick solid line), C_{RL} is $-|C_{10}|$ (thin line) and $|C_{10}|$ (thin dashed line). The coefficients of the other interactions in \mathcal{M}_{NEW} are set to zero.

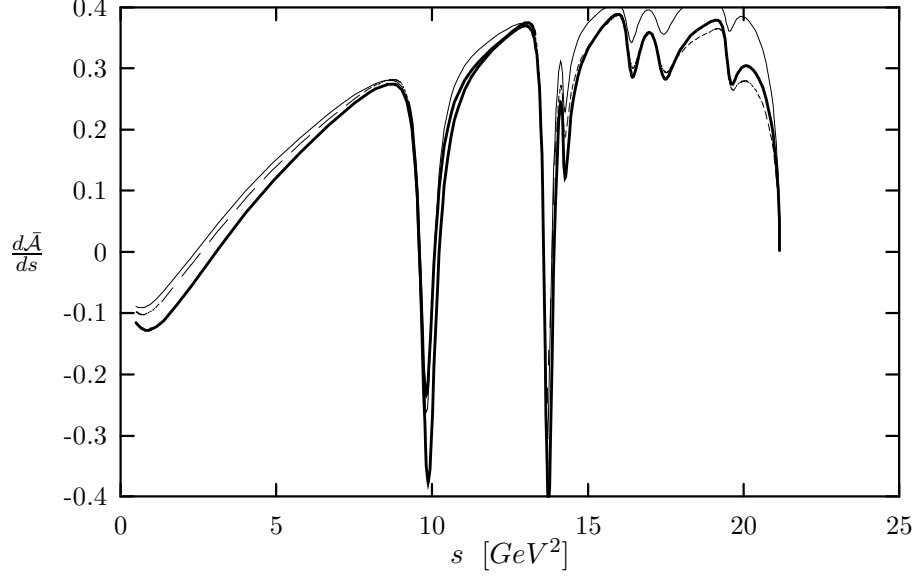


Figure 14 The normalized FB asymmetry for the SM (thick solid line), C_{RR} is $-|C_{10}|$ (thin line) and $-|C_{10}|$ (thin dashed line). The coefficients of the other interactions in \mathcal{M}_{NEW} are set to zero.

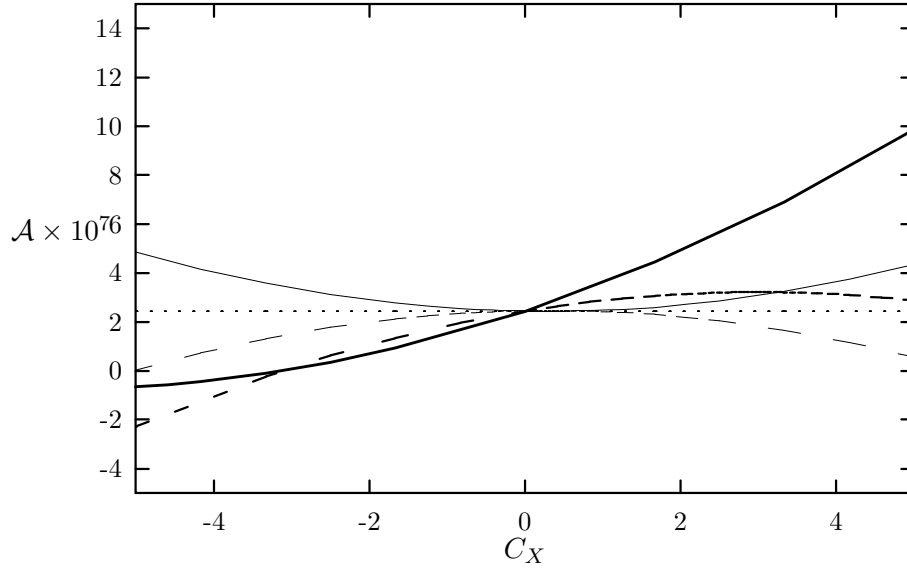


Figure 15 The contribution to the integrated FB asymmetry \mathcal{A} from C_{LL} (thick solid line), C_{LR} (thick dashed line), C_{RL} (thin dashed line), C_{RR} (thin solid line) and C_{LRRLR} (dotted line).

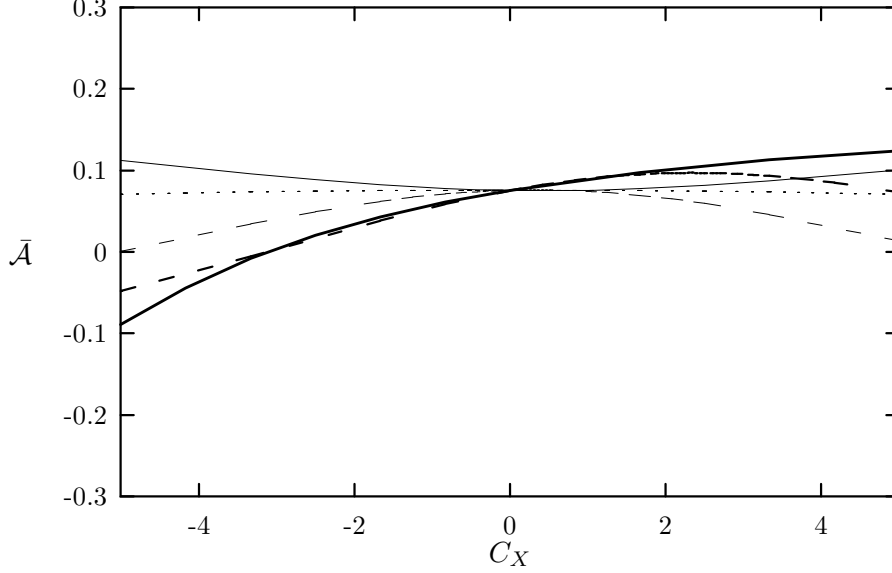


Figure 16 The contribution to the integrated normalized FB asymmetry $\bar{\mathcal{A}}$ from C_{LL} (thick solid line), C_{LR} (thick dashed line), C_{RL} (thin dashed line), C_{RR} (thin solid line) and C_{LRLR} (dotted line).

3 Correlation between the branching ratio and the forward-backward asymmetry

In the previous Sections we have studied how the branching ratios and the asymmetries depend on each interaction. In order to distinguish which interaction contributes to the process, we plot the correlation between the branching ratio and the asymmetry. By changing a coefficient, we can draw a flow in the two dimensional planes $(\mathcal{B}, \mathcal{A})$ and $(\mathcal{B}, \bar{\mathcal{A}})$. The flows depend on the type of interaction which acts. Then we may pin down the type of interaction which contributes to the processes once these quantities are measured. We allow the coefficients to vary in a wider range, *i.e.*, $-20 < C_X < 20$. The correlation plots are shown for $(\mathcal{B}, \mathcal{A})$ in Figure 17, and for $(\mathcal{B}, \bar{\mathcal{A}})$ in Figure 18. \mathcal{B} , \mathcal{A} , and $\bar{\mathcal{A}}$ are also plotted as functions of the various coefficients in the range. (See Figures 19-21.) There are uncertainties in the SM predictions which come from the renormalization point (μ) dependence of QCD correction. The predictions of the SM are shown for three values of the renormalization point. The flows in the $(\mathcal{B}, \mathcal{A})$ plane near the point of the SM prediction is summarized as follows.

- The figures show that the flow for C_{LL} is distinctive from the others. In particular, if C_{LL} is negative, the branching ratio decreases substantially while the other interactions tend to increase the branching ratio.

- As $|C_{LR}|$ and $|C_{RL}|$ increase, the asymmetry decreases except the range $0 < C_{LR} < 3$. The branching ratio tends to increase as $|C_{LR}|$ and $|C_{RL}|$ are larger.
- As $|C_{RR}|$ increases, the asymmetry and the branching ratio increase.
- The tensor and scalar interactions do not affect the asymmetry and increase the branching ratio. Therefore the flow becomes flat.
- The branching ratio and the asymmetry does not strongly depend on the sign of C_{RL} and C_{RR} . Therefore, the flow for the positive coefficient and that of the negative coefficient are nearly degenerate. The flows for the positive C_{LL} and C_{LR} are distinct from those for the negative coefficients. They are not degenerate because the branching ratio and/or the asymmetry depend on their sign.

The flow in the plane $(\mathcal{B}, \bar{\mathcal{A}})$ is similar to that in $(\mathcal{B}, \mathcal{A})$ for small changes of the coefficients. As coefficients are increased, nonlinear dependence begins to be important. This causes the difference between \mathcal{A} and $\bar{\mathcal{A}}$. As an example, increasing the coefficient of a scalar or tensor operator, in the $(\mathcal{B}, \bar{\mathcal{A}})$ plane, the asymptote of the flow is $\bar{\mathcal{A}} = 0$, while in the $(\mathcal{B}, \mathcal{A})$ plane, it is flat.

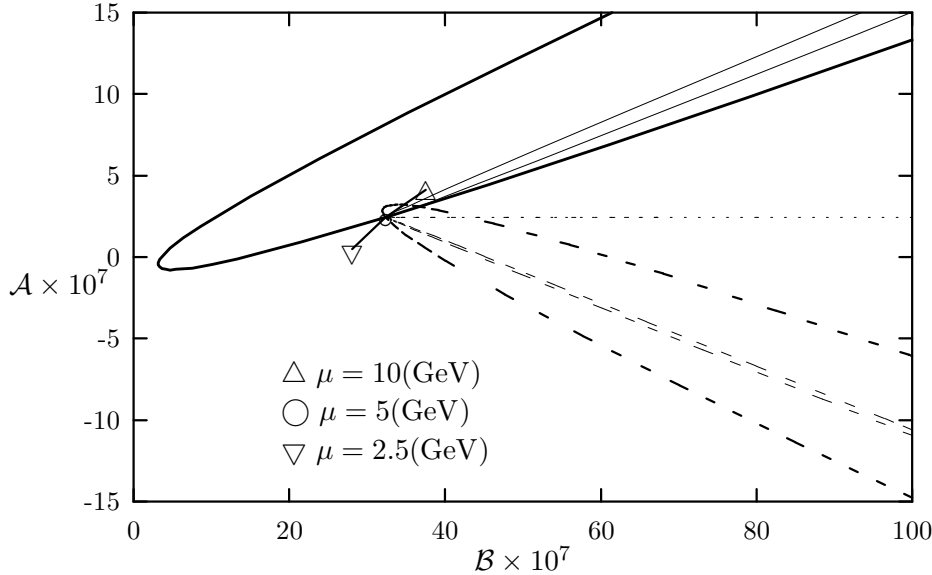


Figure 17 The flows in $(\mathcal{B}, \mathcal{A})$ plane. In each flow, C_{LL} (thick solid line), C_{LR} (thick dashed line), C_{RL} (thin dashed line), C_{RR} (thin solid line), and the tensor and scalar interactions (dotted line) are changed respectively. The predictions of the SM are denoted by \triangle , \circ , and ∇ corresponding to three values of the renormalization point (μ).

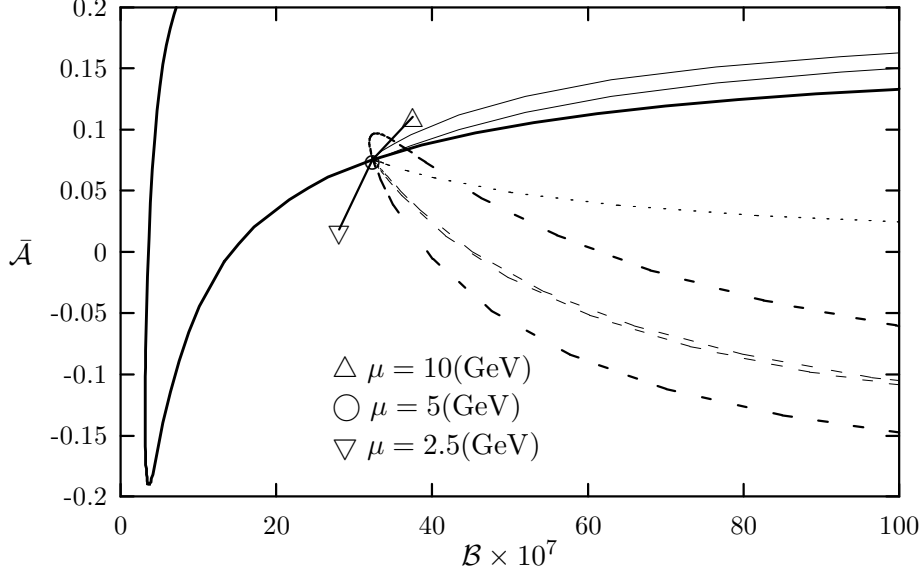


Figure 18 The flows in $(\mathcal{B}, \bar{\mathcal{A}})$ plane. In each flow, C_{LL} (thick solid line), C_{LR} (thick dashed line), C_{RL} (thin dashed line), C_{RR} (thin solid line), and the tensor and scalar interactions (dotted line) are changed respectively. The predictions of the SM are denoted as \triangle , \circ , and ∇ corresponding to three values of the renormalization point (μ).

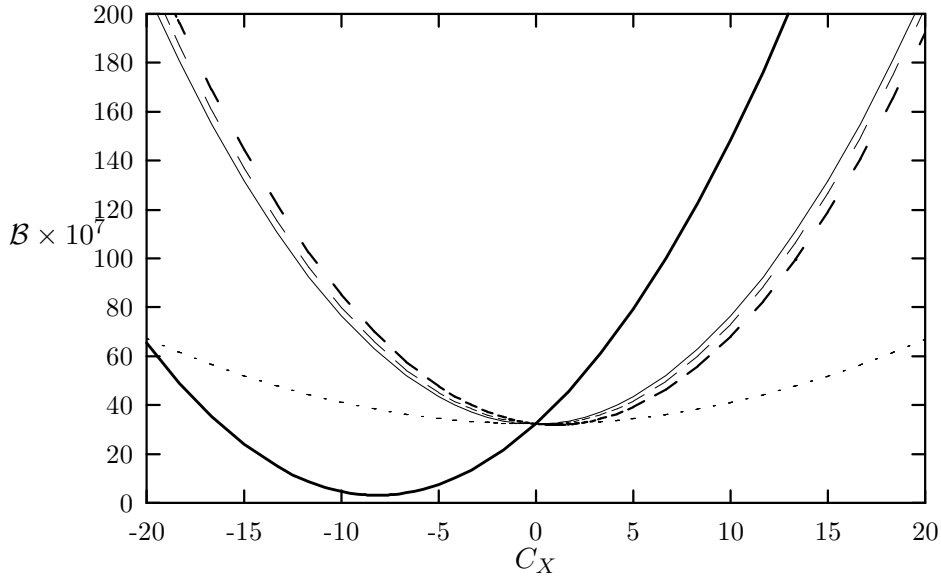


Figure 19 The partially integrated branching ratio $\mathcal{B} = \int_1^8 \frac{d\mathcal{B}}{ds} ds$ as a function of C_{LL} (thick solid line), C_{LR} (thick dashed line), C_{RL} (thin dashed line), C_{RR} (thin solid line) and C_{LRLR} (dotted line).

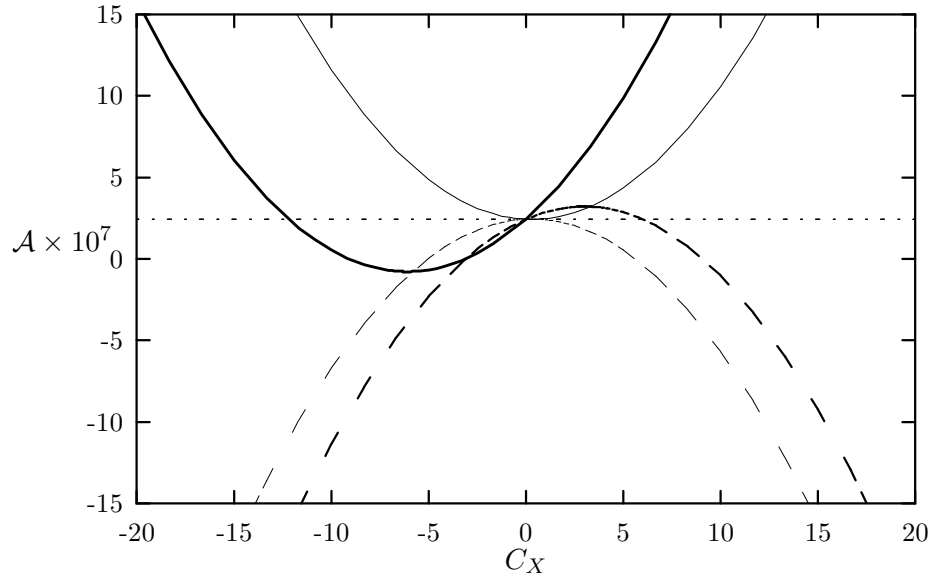


Figure 20 The contribution to the integrated FB asymmetry \mathcal{A} from C_{LL} (thick solid line), C_{LR} (thick dashed line), C_{RL} (thin dashed line), C_{RR} (thin solid line) and the tensor and scalar interactions (dotted line).

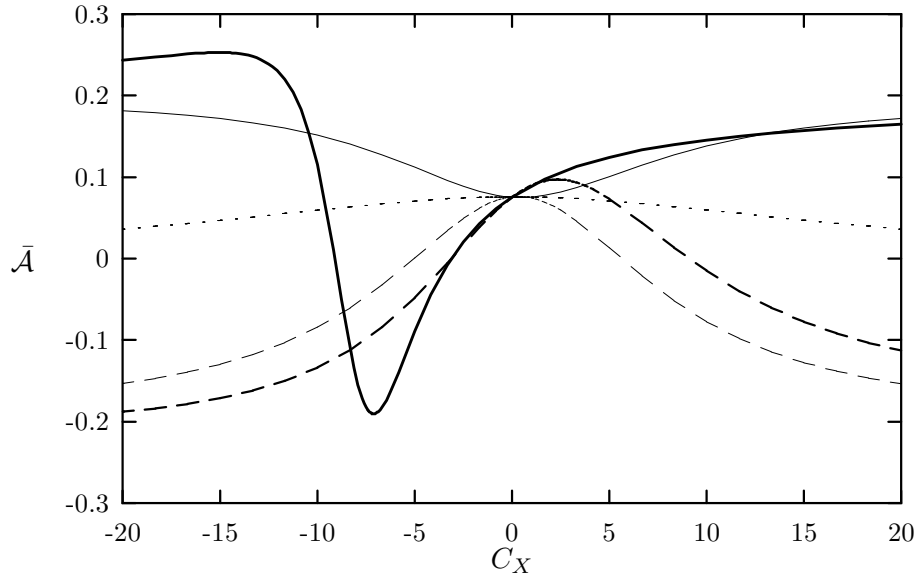


Figure 21 The contribution to the integrated normalized asymmetry $\bar{\mathcal{A}}$ from C_{LL} (thick solid line), C_{LR} (thick dashed line), C_{RL} (thin dashed line), C_{RR} (thin solid line) and the tensor and scalar interactions (dotted line).

4 Summary

We have given the most general model-independent analysis of the rare B decay process $B \rightarrow X_s l^+ l^-$. This process is experimentally very clean, and possibly most sensitive to the various extensions of the Standard Model (SM), compared to other rare decay processes. As is well known, the main reason for studying rare B decays is to measure the effective FCNC vertices in order to test the SM precisely and to search for new physics beyond the SM. We have investigated the decay $B \rightarrow X_s l^+ l^-$ in the full operator basis, instead of doing a model by model analysis. The sensitivity to the coefficients of ten independent local four-Fermi interactions is systematically studied for the branching ratios and the forward-backward (FB) asymmetries. The correlation between the branching ratio and the FB asymmetry has been studied, and the flow for C_{LL} , the coefficient of the operator $(\bar{s}_L \gamma_\mu b_L \bar{l}_L \gamma^\mu l_L)$, is found to be distinctive from the other vector type interactions. The reason for the strong sensitivity to C_{LL} comes from the large interference between $(C_9 - C_{10})$ and C_{LL} . The tensor and scalar operators increase the branching ratio, while the asymmetry is not changed at all. The other flows have also been discussed in detail.

As further comments, the uncertainties from higher-order QCD corrections can be reduced and such a reduction is very useful to distinguish the effect of new physics from the uncertainties in the predictions of the SM. Unless the theoretical predictions for the rates and the asymmetries in the SM are on firm ground, it would be difficult to make sure that new physics has indeed been discovered. A complete short distance NLO calculation for $B \rightarrow X_s l^+ l^-$ is available [14, 15], and the $1/m_b^2$ corrections have also been known [17, 19] for some time, but these are found to give only very small corrections. The remaining uncertainties are the non-perturbative long distance contributions associated with the J/ψ and ψ' resonances [22], where some modeling uncertainties remain, and the related $1/m_c^2$ corrections.

The other useful measurements, such as the tau polarization asymmetry, CP-violating rate asymmetry [23] and triple momentum-spin correlations can be studied and independent information on the coefficients can also be obtained [25]. The analysis based on a specific model may be systematically organized [25] in our scheme, because the comparison of the predictions of the various models will be easy in our framework.

Acknowledgments

We would like to thank K. Kiers, Y. Okada and A. I. Sanda for a careful reading of the manuscript and for suggestions. The work of C.S.K. was supported in part by Non-Directed-Research-Fund

of year 1997, KRF, in part by the CTP, Seoul National University, in part by the BSRI Program, Ministry of Education, BSRI-98-2425 and in part by the KOSEF-DFG large collaboration project, Project No. 96-0702-01-01-2. The work of T.M. was supported by Grant-in-Aid for Scientific Research on Priority Areas (Physics of CP violation). The work of T.Y. was supported in part by Grant-in-Aid for Scientific Research from the Ministry of Education, Science and Culture of Japan and in part by JSPS Research Fellowships for Young Scientists.

A Appendix

In this Appendix, we derive the various distributions for the massive lepton case. The formulae can be applied to the process $B \rightarrow X_s \tau^+ \tau^-$.

The double differential rate is a function of the dilepton invariant mass s and $z = \cos\theta$,

$$\begin{aligned}
\frac{d\mathcal{B}}{dsdz} = \frac{1}{2m_b^8} \mathcal{B}_0 \quad [& A_1(s, z) \{4|C_7|^2\} \\
& + A_2(s, z) \{ |(C_9^{eff} - C_{10})|^2 + |(C_9^{eff} + C_{10})|^2 \} \\
& + A_3(s, z) \{ |(C_9^{eff} - C_{10})|^2 - |(C_9^{eff} + C_{10})|^2 \} \\
& + A_4(s, z) \{ 2Re(-2C_7(C_9^{eff*} - C_{10}^*)) + 2Re(-2C_7(C_9^{eff*} + C_{10}^*)) \} \\
& + A_5(s, z) \{ 2Re(-2C_7(C_9^{eff*} - C_{10}^*)) - 2Re(-2C_7(C_9^{eff*} + C_{10}^*)) \} \\
& + L_1(s, z) \{ 2Re((C_9^{eff} - C_{10})(C_9^{eff*} + C_{10}^*)) \} \\
& + A_2(s, z) \{ 2Re((C_9^{eff} - C_{10})\mathbf{C}_{\mathbf{LL}}^*) + 2Re((C_9^{eff} + C_{10})\mathbf{C}_{\mathbf{LR}}^*) \} \\
& + A_3(s, z) \{ 2Re((C_9^{eff} - C_{10})\mathbf{C}_{\mathbf{LL}}^*) - 2Re((C_9^{eff} + C_{10})\mathbf{C}_{\mathbf{LR}}^*) \} \\
& + A_4(s, z) \{ 2Re(-2C_7(\mathbf{C}_{\mathbf{LL}}^* + \mathbf{C}_{\mathbf{LR}}^*)) \} \\
& + A_5(s, z) \{ 2Re(-2C_7(\mathbf{C}_{\mathbf{LL}}^* - \mathbf{C}_{\mathbf{LR}}^*)) \} \\
& + A_6(s, z) \{ 2Re(-2C_7(\mathbf{C}_{\mathbf{RL}}^* + \mathbf{C}_{\mathbf{RR}}^*)) \} \\
& + A_6(s, z) \{ -2Re((C_9^{eff} - C_{10})\mathbf{C}_{\mathbf{RL}}^*) - 2Re((C_9^{eff} + C_{10})\mathbf{C}_{\mathbf{RR}}^*) \} \\
& + A_7(s, z) \{ 2Re(-2C_7(\mathbf{C}_{\mathbf{RL}}^* - \mathbf{C}_{\mathbf{RR}}^*)) \} \\
& + L_2(s, z) \{ 4m_b Re(-2C_7(\mathbf{C}_{\mathbf{LRLR}}^* + \mathbf{C}_{\mathbf{LRRL}}^*)) \} \\
& + L_2(s, z) \{ 4m_s Re(-2C_7(\mathbf{C}_{\mathbf{RLLR}}^* + \mathbf{C}_{\mathbf{RLRL}}^*)) \} \\
& + L_3(s, z) \{ 2Re(-2C_7(\mathbf{C}_{\mathbf{T}}^*)) \} \\
& + L_4(s, z) \{ 2Re(-2C_7(\mathbf{C}_{\mathbf{TE}}^*)) \} \\
& + L_1(s, z) \{ 2Re((C_9^{eff} - C_{10})\mathbf{C}_{\mathbf{LR}}^*) + 2Re((C_9^{eff} + C_{10})\mathbf{C}_{\mathbf{LL}}^*) \} \\
& + L_5(s, z) \{ -2Re((C_9^{eff} - C_{10})\mathbf{C}_{\mathbf{RL}}^*) - 2Re((C_9^{eff} + C_{10})\mathbf{C}_{\mathbf{RR}}^*) \} \\
& + L_5(s, z) \{ 2Re((C_9^{eff} - C_{10})\mathbf{C}_{\mathbf{RR}}^*) + 2Re((C_9^{eff} + C_{10})\mathbf{C}_{\mathbf{RL}}^*) \} \\
& + L_6(s, z) \{ 2Re((C_9^{eff} - C_{10})(\mathbf{C}_{\mathbf{LRLR}}^* - \mathbf{C}_{\mathbf{LRRL}}^*)) \\
& \quad - 2Re((C_9^{eff} + C_{10})(\mathbf{C}_{\mathbf{LRLR}}^* - \mathbf{C}_{\mathbf{LRRL}}^*)) \} \\
& + L_2(s, z) (-m_b) \{ 2Re((C_9^{eff} - C_{10})(\mathbf{C}_{\mathbf{LRLR}}^* + \mathbf{C}_{\mathbf{LRRL}}^*)) \\
& \quad + 2Re((C_9^{eff} + C_{10})(\mathbf{C}_{\mathbf{LRLR}}^* + \mathbf{C}_{\mathbf{LRRL}}^*)) \}
\end{aligned}$$

$$\begin{aligned}
& + L_7(s, z) \{2\text{Re}((C_9^{eff} - C_{10})(\mathbf{C}_{\text{RLRL}}^* - \mathbf{C}_{\text{RLLR}}^*) \\
& \quad - 2\text{Re}((C_9^{eff} + C_{10})(\mathbf{C}_{\text{RLRL}}^* - \mathbf{C}_{\text{RLLR}}^*))\} \\
& + L_2(s, z) (-m_s) \{2\text{Re}((C_9^{eff} - C_{10})(\mathbf{C}_{\text{RLLR}}^* + \mathbf{C}_{\text{RLRL}}^*) \\
& \quad + 2\text{Re}((C_9^{eff} + C_{10})(\mathbf{C}_{\text{RLLR}}^* + \mathbf{C}_{\text{RLRL}}^*))\} \\
& + L_8(s, z) \{2\text{Re}((C_9^{eff} - C_{10})\mathbf{C}_{\text{T}}^*) + 2\text{Re}((C_9^{eff} + C_{10})\mathbf{C}_{\text{T}}^*)\} \\
& + L_2(s, z) 12(m_b + m_s) \{2\text{Re}((C_9^{eff} - C_{10})\mathbf{C}_{\text{T}}^*) - 2\text{Re}((C_9^{eff} + C_{10})\mathbf{C}_{\text{T}}^*)\} \\
& + L_9(s, z) \{2\text{Re}((C_9^{eff} - C_{10})\mathbf{C}_{\text{TE}}^*) + 2\text{Re}((C_9^{eff} + C_{10})\mathbf{C}_{\text{TE}}^*)\} \\
& + L_2(s, z) 24(-m_b + m_s) \{2\text{Re}((C_9^{eff} - C_{10})\mathbf{C}_{\text{TE}}^*) - 2\text{Re}((C_9^{eff} + C_{10})\mathbf{C}_{\text{TE}}^*)\} \\
& + A_2(s, z) \{|\mathbf{C}_{\text{LL}}|^2 + |\mathbf{C}_{\text{LR}}|^2 + |\mathbf{C}_{\text{RL}}|^2 + |\mathbf{C}_{\text{RR}}|^2\} \\
& + A_3(s, z) \{|\mathbf{C}_{\text{LL}}|^2 - |\mathbf{C}_{\text{LR}}|^2 - |\mathbf{C}_{\text{RL}}|^2 + |\mathbf{C}_{\text{RR}}|^2\} \\
& + A_6(s, z) \{-2\text{Re}(\mathbf{C}_{\text{LL}}\mathbf{C}_{\text{RL}}^* + \mathbf{C}_{\text{LR}}\mathbf{C}_{\text{RR}}^*) \\
& \quad + \text{Re}(\mathbf{C}_{\text{LRLR}}\mathbf{C}_{\text{RLLR}}^* + \mathbf{C}_{\text{LRRL}}\mathbf{C}_{\text{RLRL}}^*)\} \\
& + A_8(s, z) \{|\mathbf{C}_{\text{LRLR}}|^2 + |\mathbf{C}_{\text{RLLR}}|^2 + |\mathbf{C}_{\text{LRRL}}|^2 + |\mathbf{C}_{\text{RLRL}}|^2\} \\
& + A_3(s, z) \{-4\text{Re}(\mathbf{C}_{\text{LRLR}})(\mathbf{C}_{\text{T}}^* - 2\mathbf{C}_{\text{TE}}^*) - 4\text{Re}(\mathbf{C}_{\text{RLRL}})(\mathbf{C}_{\text{T}} + 2\mathbf{C}_{\text{TE}}^*)\} \\
& + A_9(s, z) \{16|\mathbf{C}_{\text{T}}|^2\} \\
& + A_9(s, z) \{64|\mathbf{C}_{\text{TE}}|^2\} \\
& + L_1(s, z) \{2\text{Re}(\mathbf{C}_{\text{LL}}\mathbf{C}_{\text{LR}}^* + \mathbf{C}_{\text{RL}}\mathbf{C}_{\text{RR}}^*) \\
& \quad - \text{Re}(\mathbf{C}_{\text{LRLR}}\mathbf{C}_{\text{LRRL}}^* + \mathbf{C}_{\text{RLLR}}\mathbf{C}_{\text{RLRL}}^*)\} \\
& + L_5(s, z) \{-2\text{Re}(\mathbf{C}_{\text{LL}}\mathbf{C}_{\text{RL}}^* + \mathbf{C}_{\text{LR}}\mathbf{C}_{\text{RR}}^*) \\
& \quad + \text{Re}(\mathbf{C}_{\text{LRLR}}\mathbf{C}_{\text{RLLR}}^* + \mathbf{C}_{\text{LRRL}}\mathbf{C}_{\text{RLRL}}^*)\} \\
& + L_5(s, z) \{2\text{Re}(\mathbf{C}_{\text{LL}}\mathbf{C}_{\text{RR}}^* + \mathbf{C}_{\text{LR}}\mathbf{C}_{\text{RL}}^*) \\
& \quad + \frac{1}{2}\text{Re}(\mathbf{C}_{\text{LRLR}}\mathbf{C}_{\text{RLRL}}^* + \mathbf{C}_{\text{LRRL}}\mathbf{C}_{\text{RLLR}}^*)\} \\
& + L_6(s, z) \{2\text{Re}(\mathbf{C}_{\text{LL}} - \mathbf{C}_{\text{LR}})(\mathbf{C}_{\text{LRLR}}^* - \mathbf{C}_{\text{LRRL}}^*) \\
& \quad + 2\text{Re}(\mathbf{C}_{\text{RL}} - \mathbf{C}_{\text{RR}})(\mathbf{C}_{\text{RLLR}}^* - \mathbf{C}_{\text{RLRL}}^*)\} \\
& + L_2(s, z) (-m_b) \{2\text{Re}(\mathbf{C}_{\text{LL}} + \mathbf{C}_{\text{LR}})(\mathbf{C}_{\text{LRLR}}^* + \mathbf{C}_{\text{LRRL}}^*) \\
& \quad + 2\text{Re}(\mathbf{C}_{\text{RL}} + \mathbf{C}_{\text{RR}})(\mathbf{C}_{\text{RLLR}}^* + \mathbf{C}_{\text{RLRL}}^*)\} \\
& + L_7(s, z) \{2\text{Re}(\mathbf{C}_{\text{LL}} - \mathbf{C}_{\text{LR}})(\mathbf{C}_{\text{RLRL}}^* + \mathbf{C}_{\text{RLLR}}^*) \\
& \quad + 2\text{Re}(\mathbf{C}_{\text{RL}} - \mathbf{C}_{\text{RR}})(\mathbf{C}_{\text{LRRL}}^* - \mathbf{C}_{\text{LRLR}}^*)\}
\end{aligned}$$

$$\begin{aligned}
& + L_2(s, z) (-m_s) \{2\text{Re}(\mathbf{C}_{\text{LL}} + \mathbf{C}_{\text{LR}})(\mathbf{C}_{\text{RLRL}}^* + \mathbf{C}_{\text{RLLR}}^*) \\
& \quad + 2\text{Re}(\mathbf{C}_{\text{RL}} + \mathbf{C}_{\text{RR}})(\mathbf{C}_{\text{LRRL}}^* - \mathbf{C}_{\text{LRLR}}^*)\} \\
& + L_8(s, z) \{2\text{Re}(\mathbf{C}_{\text{LL}} + \mathbf{C}_{\text{LR}})(\mathbf{C}_{\text{T}}^*) + 2\text{Re}(\mathbf{C}_{\text{RL}} + \mathbf{C}_{\text{RR}})(\mathbf{C}_{\text{T}}^*)\} \\
& + L_2(s, z) 12(m_b + m_s) \{2\text{Re}(\mathbf{C}_{\text{LL}} - \mathbf{C}_{\text{LR}})(\mathbf{C}_{\text{T}}^*) + 2\text{Re}(\mathbf{C}_{\text{RL}} - \mathbf{C}_{\text{RR}})(\mathbf{C}_{\text{T}}^*)\} \\
& + L_9(s, z) \{2\text{Re}(\mathbf{C}_{\text{LL}} + \mathbf{C}_{\text{LR}})(\mathbf{C}_{\text{TE}}^*) + 2\text{Re}(\mathbf{C}_{\text{RL}} + \mathbf{C}_{\text{RR}})(\mathbf{C}_{\text{TE}}^*)\} \\
& + L_2(s, z) 24(-m_b + m_s) \{2\text{Re}(\mathbf{C}_{\text{LL}} - \mathbf{C}_{\text{LR}})(\mathbf{C}_{\text{TE}}^*) \\
& \quad + 2\text{Re}(\mathbf{C}_{\text{RL}} - \mathbf{C}_{\text{RR}})(\mathbf{C}_{\text{TE}}^*)\} \\
& + L_5(s, z) \{-192 |\mathbf{C}_{\text{TE}}|^2\}, \tag{A-1}
\end{aligned}$$

where A_n and L_n are functions of the kinematic variables s and z ,

$$\begin{aligned}
u(s) &= \sqrt{(s - (m_b + m_s)^2)(s - (m_b - m_s)^2)(1 - \frac{4m_l^2}{s})}, \\
A_1 &= \frac{1}{s^2} u(s) [-16m_b^2 m_s^2 s (2m_l^2 + s) \\
& \quad + (m_b^2 + m_s^2) \{m_l^2 (-8(m_b^2 + m_s^2)s + 8(m_b^2 - m_s^2)^2) + 2s(-s^2 + u(s)^2 z^2 + (m_b^2 - m_s^2)^2)\}], \\
A_2 &= u(s) (-u(s)^2 z^2 - s^2 + (m_b^2 - m_s^2)^2), \\
A_3 &= 2u(s)^2 z s, \\
A_4 &= u(s) \frac{1}{s} \{2(2m_l^2 + s)((m_b^2 + m_s^2)s - (m_b^2 - m_s^2)^2), \\
A_5 &= -2(m_b^2 + m_s^2) u(s)^2 z, \\
A_6 &= 4u(s) m_b m_s (2m_l^2 + s), \\
A_7 &= 4m_b m_s u(s)^2 z, \\
A_8 &= -u(s) (m_b^2 + m_s^2 - s) (2m_l^2 - s), \\
A_9 &= u(s) \{4m_l^2 (m_b^2 - 6m_b m_s + m_s^2 - s) \\
& \quad - 2u(s)^2 z^2 - 2(m_b^2 + m_s^2)s + 2(m_b^2 - m_s^2)^2\}, \\
L_1 &= 4u(s) m_l^2 (m_b^2 + m_s^2 - s), \\
L_2 &= m_l u(s)^2 z, \\
L_3 &= u(s) \frac{1}{s} m_l (m_b + m_s) (8s^2 + 8s(m_b^2 + 6m_b m_s + m_s^2) - 16(m_b^2 - m_s^2)^2), \\
L_4 &= u(s) \frac{1}{s} m_l (m_b - m_s) (-16s^2 - 16s(m_b^2 - 6m_b m_s + m_s^2) + 32(m_b^2 - m_s^2)^2), \\
L_5 &= -16u(s) m_b m_s m_l^2, \\
L_6 &= u(s) m_l m_b (s - m_b^2 + m_s^2), \\
L_7 &= u(s) m_l m_s (s + m_b^2 - m_s^2),
\end{aligned}$$

$$\begin{aligned}
L_8 &= 12u(s)m_l(-(m_b + m_s)s + (m_b - m_s)(m_b^2 - m_s^2), \\
L_9 &= 24u(s)m_l((m_b - m_s)s - (m_b + m_s)(m_b^2 - m_s^2).
\end{aligned} \tag{A-2}$$

Among them, $A_1, A_2, A_4, A_6, A_8, A_9, L_1, L_3, L_4, L_5, L_6, L_7, L_8$ and L_9 are even functions with respect to z , while A_3, A_5, A_7, L_2 are odd functions. In the limit of $m_l = 0$, L_n vanish and A_n lead to those in the massless limit.

To investigate the differential decay rate and the FB asymmetry, we define the following functions. They are obtained by integrateing the $A_n(s, z)$ (n is 1 to 9) and $L_n(s, z)$ with respect to z as follows,

$$\begin{aligned}
M_i(s) &= \int_{-1}^1 A_i(s, z) dz = 2A_i(s, \sqrt{1/3}), \\
N_j(s) &= \int_{-1}^1 L_j(s, z) dz = 2L_j(s, \sqrt{1/3}),
\end{aligned} \tag{A-3}$$

where i is 1,2,4,6,8 and 9, and j is 1,3,4,5,6,7,8 and 9. Also

$$\begin{aligned}
A_k(s, 1) &= \int_0^1 A_k(s, z) dz - \int_{-1}^0 A_k(s, z) dz, \\
L_2(s, 1) &= \int_0^1 L_2(s, z) dz - \int_{-1}^0 L_2(s, z) dz,
\end{aligned} \tag{A-4}$$

where k is 3,5 and 7.

Finally, the differential decay rate is given by

$$\begin{aligned}
\frac{d\mathcal{B}}{ds} = \frac{1}{2m_b^8} \mathcal{B}_0 & [M_1(s) \{4|C_7|^2\} \\
& + M_2(s) \{ |(C_9^{eff} - C_{10})|^2 + |(C_9^{eff} + C_{10})|^2 \} \\
& + M_4(s) \{ 2Re(-2C_7(C_9^{eff*} - C_{10}^*)) + 2Re(-2C_7(C_9^{eff*} + C_{10}^*)) \} \\
& + N_1(s) \{ 2Re((C_9^{eff} - C_{10})(C_9^{eff*} + C_{10}^*)) \} \\
& + M_2(s) \{ 2Re((C_9^{eff} - C_{10})\mathbf{C}_{\mathbf{LL}}^*) + 2Re((C_9^{eff} + C_{10})\mathbf{C}_{\mathbf{LR}}^*) \} \\
& + M_4(s) \{ 2Re(-2C_7(\mathbf{C}_{\mathbf{LL}}^* + \mathbf{C}_{\mathbf{LR}}^*)) \} \\
& + M_6(s) \{ 2Re(-2C_7(\mathbf{C}_{\mathbf{RL}}^* + \mathbf{C}_{\mathbf{RR}}^*)) \} \\
& + M_6(s) \{ -2Re((C_9^{eff} - C_{10})\mathbf{C}_{\mathbf{RL}}^*) - 2Re((C_9^{eff} + C_{10})\mathbf{C}_{\mathbf{RR}}^*) \} \\
& + N_3(s) \{ 2Re(-2C_7(\mathbf{C}_{\mathbf{T}}^*)) \} \\
& + N_4(s) \{ 2Re(-2C_7(\mathbf{C}_{\mathbf{TE}}^*)) \} \\
& + N_1(s) \{ 2Re((C_9^{eff} - C_{10})\mathbf{C}_{\mathbf{LR}}^*) + 2Re((C_9^{eff} + C_{10})\mathbf{C}_{\mathbf{LL}}^*) \} \\
& + N_5(s) \{ -2Re((C_9^{eff} - C_{10})\mathbf{C}_{\mathbf{RL}}^*) - 2Re((C_9^{eff} + C_{10})\mathbf{C}_{\mathbf{RR}}^*) \}
\end{aligned}$$

$$\begin{aligned}
& + N_5(s) \{2\text{Re}((C_9^{eff} - C_{10})\mathbf{C}_{\mathbf{RR}}^*) + 2\text{Re}((C_9^{eff} + C_{10})\mathbf{C}_{\mathbf{RL}}^*)\} \\
& + N_6(s) \{2\text{Re}((C_9^{eff} - C_{10})(\mathbf{C}_{\mathbf{LRLR}}^* - \mathbf{C}_{\mathbf{LRRL}}^*)) \\
& \quad - 2\text{Re}((C_9^{eff} + C_{10})(\mathbf{C}_{\mathbf{LRLR}}^* - \mathbf{C}_{\mathbf{LRRL}}^*))\} \\
& + N_7(s) \{2\text{Re}((C_9^{eff} - C_{10})(\mathbf{C}_{\mathbf{RLRL}}^* - \mathbf{C}_{\mathbf{RLLR}}^*)) \\
& \quad - 2\text{Re}((C_9^{eff} + C_{10})(\mathbf{C}_{\mathbf{RLRL}}^* - \mathbf{C}_{\mathbf{RLLR}}^*))\} \\
& + N_8(s) \{2\text{Re}((C_9^{eff} - C_{10})\mathbf{C}_{\mathbf{T}}^*) + 2\text{Re}((C_9^{eff} + C_{10})\mathbf{C}_{\mathbf{T}}^*)\} \\
& + N_9(s) \{2\text{Re}((C_9^{eff} - C_{10})\mathbf{C}_{\mathbf{TE}}^*) + 2\text{Re}((C_9^{eff} + C_{10})\mathbf{C}_{\mathbf{TE}}^*)\} \\
& + M_2(s) \{|\mathbf{C}_{\mathbf{LL}}|^2 + |\mathbf{C}_{\mathbf{LR}}|^2 + |\mathbf{C}_{\mathbf{RL}}|^2 + |\mathbf{C}_{\mathbf{RR}}|^2\} \\
& + M_6(s) \{-2\text{Re}(\mathbf{C}_{\mathbf{LL}}\mathbf{C}_{\mathbf{RL}}^* + \mathbf{C}_{\mathbf{LR}}\mathbf{C}_{\mathbf{RR}}^*) \\
& \quad + \text{Re}(\mathbf{C}_{\mathbf{LRLR}}\mathbf{C}_{\mathbf{RLLR}}^* + \mathbf{C}_{\mathbf{LRRL}}\mathbf{C}_{\mathbf{RLRL}}^*)\} \\
& + M_8(s) \{|\mathbf{C}_{\mathbf{LRLR}}|^2 + |\mathbf{C}_{\mathbf{RLLR}}|^2 + |\mathbf{C}_{\mathbf{LRRL}}|^2 + |\mathbf{C}_{\mathbf{RLRL}}|^2\} \\
& + M_9(s) \{16|\mathbf{C}_{\mathbf{T}}|^2\} \\
& + M_{10}(s) \{64|\mathbf{C}_{\mathbf{TE}}|^2\} \\
& + N_1(s) \{2\text{Re}(\mathbf{C}_{\mathbf{LL}}\mathbf{C}_{\mathbf{LR}}^* + \mathbf{C}_{\mathbf{RL}}\mathbf{C}_{\mathbf{RR}}^*) \\
& \quad - \text{Re}(\mathbf{C}_{\mathbf{LRLR}}\mathbf{C}_{\mathbf{LRRL}}^* + \mathbf{C}_{\mathbf{RLLR}}\mathbf{C}_{\mathbf{RLRL}}^*)\} \\
& + N_5(s) \{-2\text{Re}(\mathbf{C}_{\mathbf{LL}}\mathbf{C}_{\mathbf{RL}}^* + \mathbf{C}_{\mathbf{LR}}\mathbf{C}_{\mathbf{RR}}^*) \\
& \quad + \text{Re}(\mathbf{C}_{\mathbf{LRLR}}\mathbf{C}_{\mathbf{RLLR}}^* + \mathbf{C}_{\mathbf{LRRL}}\mathbf{C}_{\mathbf{RLRL}}^*)\} \\
& + N_5(s) \{2\text{Re}(\mathbf{C}_{\mathbf{LL}}\mathbf{C}_{\mathbf{RR}}^* + \mathbf{C}_{\mathbf{LR}}\mathbf{C}_{\mathbf{RL}}^*) \\
& \quad + \frac{1}{2}\text{Re}(\mathbf{C}_{\mathbf{LRLR}}\mathbf{C}_{\mathbf{RLRL}}^* + \mathbf{C}_{\mathbf{LRRL}}\mathbf{C}_{\mathbf{RLLR}}^*)\} \\
& + N_6(s) \{2\text{Re}(\mathbf{C}_{\mathbf{LL}} - \mathbf{C}_{\mathbf{LR}})(\mathbf{C}_{\mathbf{LRLR}}^* - \mathbf{C}_{\mathbf{LRRL}}^*) \\
& \quad + 2\text{Re}(\mathbf{C}_{\mathbf{RL}} - \mathbf{C}_{\mathbf{RR}})(\mathbf{C}_{\mathbf{RLLR}}^* - \mathbf{C}_{\mathbf{RLRL}}^*)\} \\
& + N_7(s) \{2\text{Re}(\mathbf{C}_{\mathbf{LL}} - \mathbf{C}_{\mathbf{LR}})(\mathbf{C}_{\mathbf{RLRL}}^* + \mathbf{C}_{\mathbf{RLLR}}^*) \\
& \quad + 2\text{Re}(\mathbf{C}_{\mathbf{RL}} - \mathbf{C}_{\mathbf{RR}})(\mathbf{C}_{\mathbf{LRRL}}^* - \mathbf{C}_{\mathbf{LRLR}}^*)\} \\
& + N_8(s) \{2\text{Re}(\mathbf{C}_{\mathbf{LL}} + \mathbf{C}_{\mathbf{LR}})(\mathbf{C}_{\mathbf{T}}^*) + 2\text{Re}(\mathbf{C}_{\mathbf{RL}} + \mathbf{C}_{\mathbf{RR}})(\mathbf{C}_{\mathbf{T}}^*)\} \\
& + N_9(s) \{2\text{Re}(\mathbf{C}_{\mathbf{LL}} + \mathbf{C}_{\mathbf{LR}})(\mathbf{C}_{\mathbf{TE}}^*) + 2\text{Re}(\mathbf{C}_{\mathbf{RL}} + \mathbf{C}_{\mathbf{RR}})(\mathbf{C}_{\mathbf{TE}}^*)\} \\
& + N_{10}(s) \{-192|\mathbf{C}_{\mathbf{TE}}|^2\}. \tag{A-5}
\end{aligned}$$

And the FB asymmetry is

$$\begin{aligned}
\frac{dA}{ds} = \frac{1}{2m_b s} \mathcal{B}_0 \quad [& A_3(s, 1) \{ |(C_9^{eff} - C_{10})|^2 - |(C_9^{eff} + C_{10})|^2 \} \\
& + A_5(s, 1) \{ 2Re(-2C_7(C_9^{eff*} - C_{10}^*)) - 2Re(-2C_7(C_9^{eff*} + C_{10}^*)) \} \\
& + A_3(s, 1) \{ 2Re((C_9^{eff} - C_{10})\mathbf{C}_{LL}^*) - 2Re((C_9^{eff} + C_{10})\mathbf{C}_{LR}^*) \} \\
& + A_5(s, 1) \{ 2Re(-2C_7(\mathbf{C}_{LL}^* - \mathbf{C}_{LR}^*)) \} \\
& + A_7(s, 1) \{ 2Re(-2C_7(\mathbf{C}_{RL}^* - \mathbf{C}_{RR}^*)) \} \\
& + L_2(s, 1) \{ 4m_b Re(-2C_7(\mathbf{C}_{LRLR}^* + \mathbf{C}_{LRRR}^*)) \} \\
& + L_2(s, 1) \{ 4m_s Re(-2C_7(\mathbf{C}_{RLLR}^* + \mathbf{C}_{RLRL}^*)) \} \\
& + L_2(s, 1) (-m_b) \{ 2Re((C_9^{eff} - C_{10})(\mathbf{C}_{LRLR}^* + \mathbf{C}_{LRRR}^*)) \\
& \quad + 2Re((C_9^{eff} + C_{10})(\mathbf{C}_{LRLR}^* + \mathbf{C}_{LRRR}^*)) \} \\
& + L_2(s, 1) (-m_s) \{ 2Re((C_9^{eff} - C_{10})(\mathbf{C}_{RLLR}^* + \mathbf{C}_{RLRL}^*)) \\
& \quad + 2Re((C_9^{eff} + C_{10})(\mathbf{C}_{RLLR}^* + \mathbf{C}_{RLRL}^*)) \} \\
& + L_2(s, 1) 12(m_b + m_s) \{ 2Re((C_9^{eff} - C_{10})\mathbf{C}_T^*) - 2Re((C_9^{eff} + C_{10})\mathbf{C}_T^*) \} \\
& + L_2(s, 1) 24(-m_b + m_s) \{ 2Re((C_9^{eff} - C_{10})\mathbf{C}_{TE}^*) - 2Re((C_9^{eff} + C_{10})\mathbf{C}_{TE}^*) \} \\
& + A_3(s, 1) \{ |\mathbf{C}_{LL}|^2 - |\mathbf{C}_{LR}|^2 - |\mathbf{C}_{RL}|^2 + |\mathbf{C}_{RR}|^2 \} \\
& + A_3(s, 1) \{ -4\text{Re}(\mathbf{C}_{LRLR})(\mathbf{C}_T^* - 2\mathbf{C}_{TE}^*) - 4\text{Re}(\mathbf{C}_{RLRL})(\mathbf{C}_T^* + 2\mathbf{C}_{TE}^*) \} \\
& + L_2(s, 1) (-m_b) \{ 2\text{Re}(\mathbf{C}_{LL} + \mathbf{C}_{LR})(\mathbf{C}_{LRLR}^* + \mathbf{C}_{LRRR}^*) \\
& \quad + 2\text{Re}(\mathbf{C}_{RL} + \mathbf{C}_{RR})(\mathbf{C}_{RLLR}^* + \mathbf{C}_{RLRL}^*) \} \\
& + L_2(s, 1) (-m_s) \{ 2\text{Re}(\mathbf{C}_{LL} + \mathbf{C}_{LR})(\mathbf{C}_{RLLR}^* + \mathbf{C}_{RLRL}^*) \\
& \quad + 2\text{Re}(\mathbf{C}_{RL} + \mathbf{C}_{RR})(\mathbf{C}_{LRLR}^* + \mathbf{C}_{LRRR}^*) \} \\
& + L_2(s, 1) 12(m_b + m_s) \{ 2\text{Re}(\mathbf{C}_{LL} - \mathbf{C}_{LR})(\mathbf{C}_T^*) + 2\text{Re}(\mathbf{C}_{RL} - \mathbf{C}_{RR})(\mathbf{C}_T^*) \} \\
& + L_2(s, 1) 24(-m_b + m_s) \{ 2\text{Re}(\mathbf{C}_{LL} - \mathbf{C}_{LR})(\mathbf{C}_{TE}^*) \\
& \quad + 2\text{Re}(\mathbf{C}_{RL} - \mathbf{C}_{RR})(\mathbf{C}_{TE}^*) \} \}. \tag{A-6}
\end{aligned}$$

References

- [1] T. Goto, Y. Okada, Y. Shimizu, and M. Tanaka, Phys. Rev. **D55** (1997) 4273; T. Goto, Y. Okada, Y. Shimizu, KEK-TH-567, (hep-ph/9804294).
- [2] J. L. Hewett and J. D. Wells, Phys. Rev. **D55** (1997) 5549.
- [3] L. T. Handoko, Phys. Rev. **D57** (1998) 1776.
- [4] C. Greub, A. Ioannissian and D. Wyler, Phys. Lett. **B346** (1995) 149.
- [5] Y. Grossman, Z. Ligeti and E. Nardi, Phys. Rev. **D55** (1997) 2768.
- [6] T. G. Rizzo, SLAC-PUB-7702, (hep-ph/9802401).
- [7] Ji-Ho Jang, Y.G. Kim and J. S. Lee, KAIST-TH 97/21, (hep-ph/9711504).
- [8] P. Cho, M. Misiak, and D. Wyler, Phys. Rev. **D54** (1996) 3329.
- [9] A. Ali, G. F. Guidice, and T. Mannel, Z. Phys. **C67** (1995) 417.
- [10] J. L. Hewett, Phys. Rev. **D53** (1996) 4964.
- [11] T. Inami and C. S. Lim, Prog. Theo. Phys. **65** (1981) 297; **65** (1981) (E) 1772.
- [12] W. Hou, R.S. Willey, and A. Soni, Phys. Rev. Lett. **58** (1987) 1608 and erratum *ibid* **60** (1988) 2337.
- [13] B. Grinstein, M. Savage, M. Wise, Nucl. Phys. **B319** (1989) 271.
- [14] M. Misiak, Nucl. Phys. **B393** (1993) 23 and erratum *ibid* **B439** (1995) 461.
- [15] A. J. Buras and M. Münz, Phys. Rev. **D52** (1995) 186.
- [16] L. Michel, Proc. Phys. Soc. **A63** (1950) 514.
- [17] A. Ali, T. Mannel and T. Morozumi, Phys. Lett. **B273** (1991) 505.
- [18] The authors would like to thank Y. Okada for suggesting to them to draw the correlation.
- [19] A. Falk, M. Luke and M. J. Savage, Phys. Rev. **D49** (1994) 3367.
- [20] A. Ali, G. Hiller, L. Handoko and T. Morozumi, Phys. Rev. **D55** (1997) 4105.

- [21] C. S. Kim, T. Morozumi and A. I. Sanda, Phys. Rev. **D56** (1997) 7240; T. M. Aliev, C. S. Kim and M. Savci, YUMS-98-008, (hep-ph/9804456).
- [22] C. S. Lim, T. Morozumi and A. I. Sanda, Phys. Lett. **B218** (1989) 343; N. G. Deshpande, J. Trampetic and K. Panose, Phys. Rev. **D39** (1989) 1461; P. J. O'Donnell and H. K. K. Tung, Phys. Rev. **D43** (1991) R2067; N. Paver and Riazuddin, Phys. Rev. **D45** (1992) 978.
- [23] F. Krüger and L. M. Sehgal, Phys. Rev. **D55** (1997) 2799.
- [24] C. S. Kim and A. D. Martin, Phys. Lett. **B225** (1989) 186.
- [25] S. Fukae, C. S. Kim, T. Morozumi and T. Yoshikawa, work in progress.